CLM-R273

CLM-R273

Initial examinations of the Weldability, Creep Properties, Tempering Response and Grain Size Control in Low-Activation Martensitic Stainless Steels

K. W. Tupholme
D. Dulieu
G. J. Butterworth

UK ATOMIC ENERGY AUTHORITY

Culham Laboratory

CLM-R273

Initial Examinations of the Weldability, Creep Properties, Tempering Response and Grain Size Control in Low-Activation Martensitic Stainless Steels

K.W. Tupholme[†], D. Dulieu[†] and G.J. Butterworth[*]

[†] British Steel Corporation Swinden Laboratories
Moorgate, Rotherham, S60 3AR

[*] Culham Laboratory, Abingdon, Oxon., OX14 3DB
(Euratom/UKAEA Fusion Association)

Abstract

Earlier work has identified low-activation martensitic stainless steel compositions having properties comparable to those of commercial 12%CrMoVNb steel. The welding characteristics, creep properties, additional mechanical properties and grain refinement techniques have been examined for these steels. Welding trials show that the LA7 alloy (11Cr-3W-0.2V) can be welded using TIG methods with preheat and post-weld stress relief heat treatment. Creep tests, which are still in progress, so far indicate that the steels LA7 and LA13 (9Cr-3W-0.25V) have higher creep strain rates and possibly lower rupture strengths than FV448 steel. An evaluation of the mechanical properties of some lower alloy content low-activation steels indicated that, as expected, the steels possessed lower strength coupled with an enhanced toughness. It has been demonstrated that grain refinement can be accomplished by means of tantalum additions, though the quantitative basis for the effect of grain refining additions remains to be established. There are strong indications that the soluble nitrogen content, possibly interacting with the manganese present, influences the delta ferrite content.

Culham Laboratory
United Kingdom Atomic Energy Authority
Abingdon
Oxfordshire OX14 3DB

March 1987

ISBN: 0 85311 1626
Price: £5.00
Available from H.M. Stationery Office

CONTENTS

1. INTRODUCTION

An earlier report [1] presented the results of an initial study of a range of 9-11%Cr,V,W martensitic stainless steels designed as low-activation alloys for fusion reactor applications. The properties of these low-activation (LA) compositions were assessed relative to those obtained with the commercial martensitic CrMoNbV steel FV448. The earlier work established the strengthening effects of additions of vanadium and tungsten, principally after hardening and tempering for 2 hours at 675°C.

It was found that a close approach to the strength of the commercial steel could be obtained in an 11%Cr, 0.23%V, 3.0%W composition, designated LA7 in the earlier programme. This material, however, had a substantially coarser prior austenite grain structure than the niobium-bearing FV448 steel. It also exhibited a lower impact toughness and there was concern that the solid solution strengthening from the tungsten would be lost on overageing, as a consequence of the precipitation of a Laves type M_2X (Fe_2W) phase. In addition, it was considered that the choice of 675°C for the tempering temperature, while typical of that required to develop a high strength in the FV448 steel, was not consistent with the attainment of a toughness level adequate for reactor application. By analogy with work on HTR materials it was thought that temperatures up to 750°C might be used to improve the toughness.

In the light of these earlier findings the behaviour of the low-activation compositions has been further explored. The work reported here falls into four topic areas which are listed below in order of those involving, firstly, experimental alloys from the earlier programme and, secondly, the examination of new experimental compositions:

1. The response of LA7 steel to welding.

2. The creep rupture properties of the LA7 composition, in comparison with those of the FV448 steel.

3. The properties of selected steels from the original programme, after tempering at higher temperatures for improvement of toughness.

4. An examination of austenite grain refining agents suitable for low-activation compositions.

To maintain continuity the numbering system for casts adopted earlier has been retained. Thus Steels 1-13, with the prefix LA added to denote a low-activation composition, are those described in more detail in an earlier report [1]. For convenience, the chemical compositions of all the steels examined in the present programme are given in Table 1.

2. PRELIMINARY EXAMINATION OF THE WELDABILITY OF STEEL LA7

Welding fabrication is regarded as essential for the manufacture of first wall and blanket structures. Whilst a full assessment of the welding characteristics under realistic conditions is a major task, it was

Table 1

Chemical analysis of experimental steels, mass percent

Steel	C	Si	Mn	Cr	Mo	Ni	N	Nb	V	W
FV448	0.15	0.26	0.88	11.3	0.66	0.75	0.057	0.3	0.25	<0.02
LA4	0.17	0.45	0.78	10.9	<0.01	0.02	0.060	<0.01	0.25	0.65
LA7	0.17	0.44	0.76	11.2	0.02	<0.02	0.068	<0.01	0.23	3.04
LA8	0.16	0.47	0.78	11.1	<0.01	<0.02	0.069	<0.01	0.46	0.66
LA12	0.16	0.37	0.79	9.1	<0.02	<0.02	0.060	<0.01	0.24	0.68
LA13	0.17	0.42	0.74	9.22	0.02	<0.02	0.059	<0.01	0.25	2.90

CR 87.28/1

considered useful to conduct some preliminary studies on steel LA7 in the form of relatively thin strip. For this purpose samples of the existing 19mm bar stock were hot rolled to produce strips nominally 2mm and 5mm thick. Since there was no information on the welding characteristics of this composition, it was decided to concentrate on the properties obtained in the fusion zone. To minimise problems associated with the parent metal, a low strength structure was obtained by reducing the austenitising temperature. It was believed that the associated refinement in prior austenite grain size would be helpful in raising the toughness of the parent metal. Accordingly, the strips were hardened by air cooling after austenitising at 900°C and then tempered for 1h at 675°C.

2.1 Welding techniques

2.1.1 Autogenous welding

The 2mm thick strip was welded autogeneously. In this method an electric arc struck between a tungsten electrode and the metal melts the latter at the edges of the weld and the liquid on cooling solidifies to complete the join without the use of additional metal filler. The molten metal pool is shielded by an inert gas, in this case argon, hence the process is known as tungsten-inert-gas (TIG) welding. A minimum preheat of 200°C was specified to minimise the risk of post-weld cracking. The actual preheat temperatures and the welding conditions employed are given in Table 2.

2.1.2 TIG welding with filler

The 5mm thick strip was welded with a filler wire made by cutting wire of square section from the 2mm strip. A conventional 70° V butt weld preparation was employed, as illustrated in Fig.1. The butt weld was made with successive runs under the conditions given in Table 2 and with a minimum preheat of 200°C.

With both of the above techniques, the strip was given a stress relief treatment of 3h at 650°C immediately following the welding operation.

Table 2

Welding conditions for LA7 steel strip

weldment description	run no.	current A	voltage	preheat temperature °C
Trials on 2mm strip		85 70 50	12 12 11	229 229 229
2mm strip bend specimen		50	11	219
2mm strip tensile specimen		50	11	229
5mm strip bend specimen	1 2 3 4	75 90 95 85	12 11 11 12	230 250 (interpass)
Tensile specimen	1 2 3 4	60 80 110 95	11 12 12 12	220 250 (interpass)

CR 87.28/2

Shielding gas: 99.999% pure argon;
flow rate: 16 litre/min for the torch, 14 litre/min for the purge

2.2 Examination and testing of the welds

Flat tensile test specimens were prepared from welded strip of both thicknesses, with the weld lying transversely within the gauge length. Bend test pieces were also prepared with the weld at the centreline, perpendicular to the axis of bending. The configurations of these test pieces are shown in Fig.1.

The welds were also examined metallographically and the hardness profiles across the weld zones determined.

2.3 Test and examination results

The tensile properties of the welded and stress-relieved strips are summarised by the data shown in Table 3 and compared with the earlier results of the tests on 19mm bar of the same material. There was a substantial loss of strength in the parent metal as a consequence of the low austenitising temperature but the welds were sufficiently sound for failure to have occurred fully within the parent metal portion of the gauge length.

On free bend testing, the 2mm thick strip could be bent through 180° without cracking. The 5mm thick material could be bent to an angle of only 50° before cracking from the weld line.

A hardness profile, measured using a Vickers indentor with a 30kg load, was

(a) Weld trials on 2mm strip

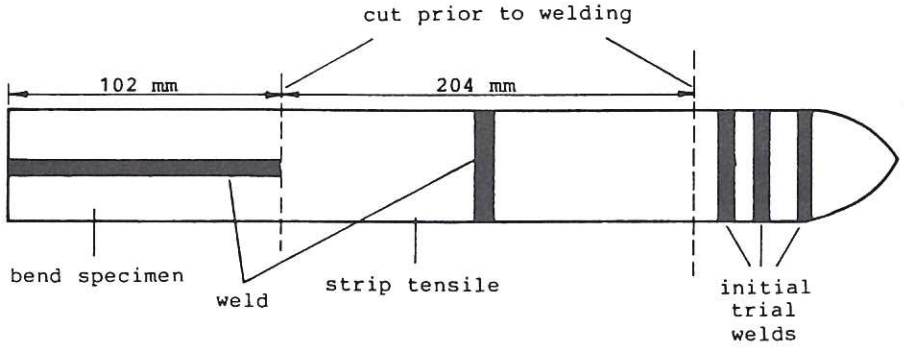

(b) Weld trials on 5mm strip

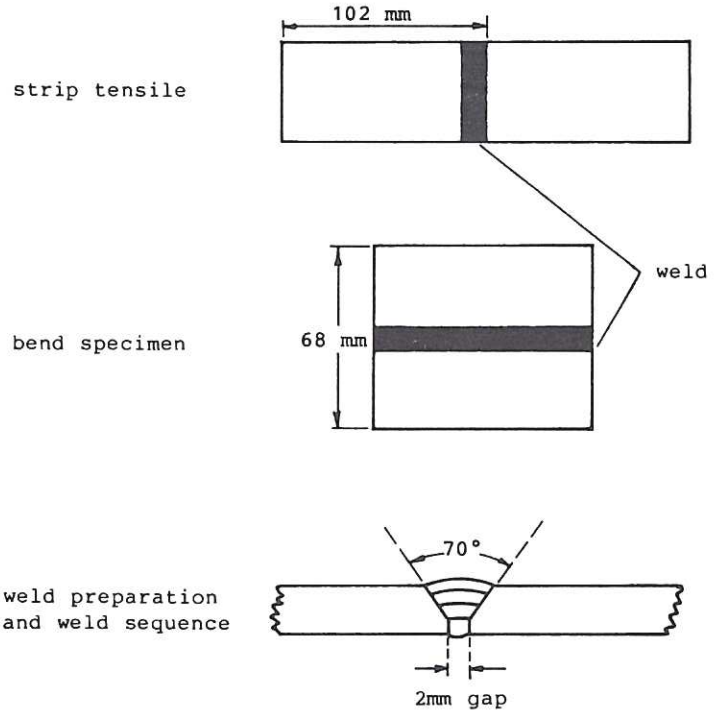

Fig.1 Configurations of the weld trials on 2 mm and 5 mm strip

Table 3

Tensile properties of welded strip samples

strip thickness mm	0.2% PS MPa	tensile strength MPa	elongation %
2mm	680	856	12
5mm	637	830	16
19mm bar (for comparison)	838	1022	14

CR87.28/3

obtained across the welds. In the case of the 2mm plate, profiles were taken before and after a stress relief treatment of 3h at 650°C. This 5mm thick strip was tested only after the stress relief treatment. The hardness profiles are shown in Figs.2-4. In the as-welded 2mm strip, the metal in the fusion line was, at 520-560 HV30, of comparable hardness to the 19mm bar sample on hardening from 1100°C. The hardness value was reduced to 320-340 HV30 by the stress relief treatment, which also softened the parent strip from 280 to 250-260 HV30.

Metallographic examination indicated that the fusion line structure was free from cracks or visible porosity and consisted of martensite with a small proportion of delta ferrite, estimated at about 6% volume fraction in both strips, as illustrated by Fig.5. As is shown by Figs.5b and 5c, isolated delta ferrite grains were relatively large. In the welds the austenite grain sizes lay in the range ASTM 6.5-7, as compared with the finer grain size of 8.5-9 in the parent strip.

2.4 Discussion of weldability of LA7

The trials have demonstrated that, once the basic welding parameters have been established, the TIG autogenous and filler processes can readily be applied to the LA7 composition. No unusual problems were encountered in the welding operation itself.

The hardness profiles of the as-welded material showed clearly the need for a post-weld heat treatment in this class of alloy. This treatment will be required when welding any high strength 9-12%Cr martensitic steel.

The absence of any porosity on the microscale is encouraging, indicating that the relatively high nitrogen content can be tolerated in these welding processes.

The formation of delta ferrite in the fusion zone indicates a problem with the LA7 composition. The difficulty may be overcome through the use of a welding rod or wire the composition of which is adjusted to compensate for any changes, such as a loss of nitrogen, that occur during welding. The formulation of a suitable consumable will, however, depend on the final choice of parent metal composition.

3. DETERMINATION OF THE CREEP RUPTURE PROPERTIES OF LA7 AND LA13 STEELS

A limited creep testing programme was pursued to determine the rupture strength and creep strain rates of the 9% and 11%Cr, 0.25%V, 3.0%W low-activation steels for comparison with the experimental cast of the FV448 composition. The primary aim was to gain both an indication of the stability of the high-tungsten steels against stress-induced structural changes and to compare their performance with that of the standard material.

The limitations imposed by radiation damage on the service life of fusion reactor components imply that the long-term creep properties are of little

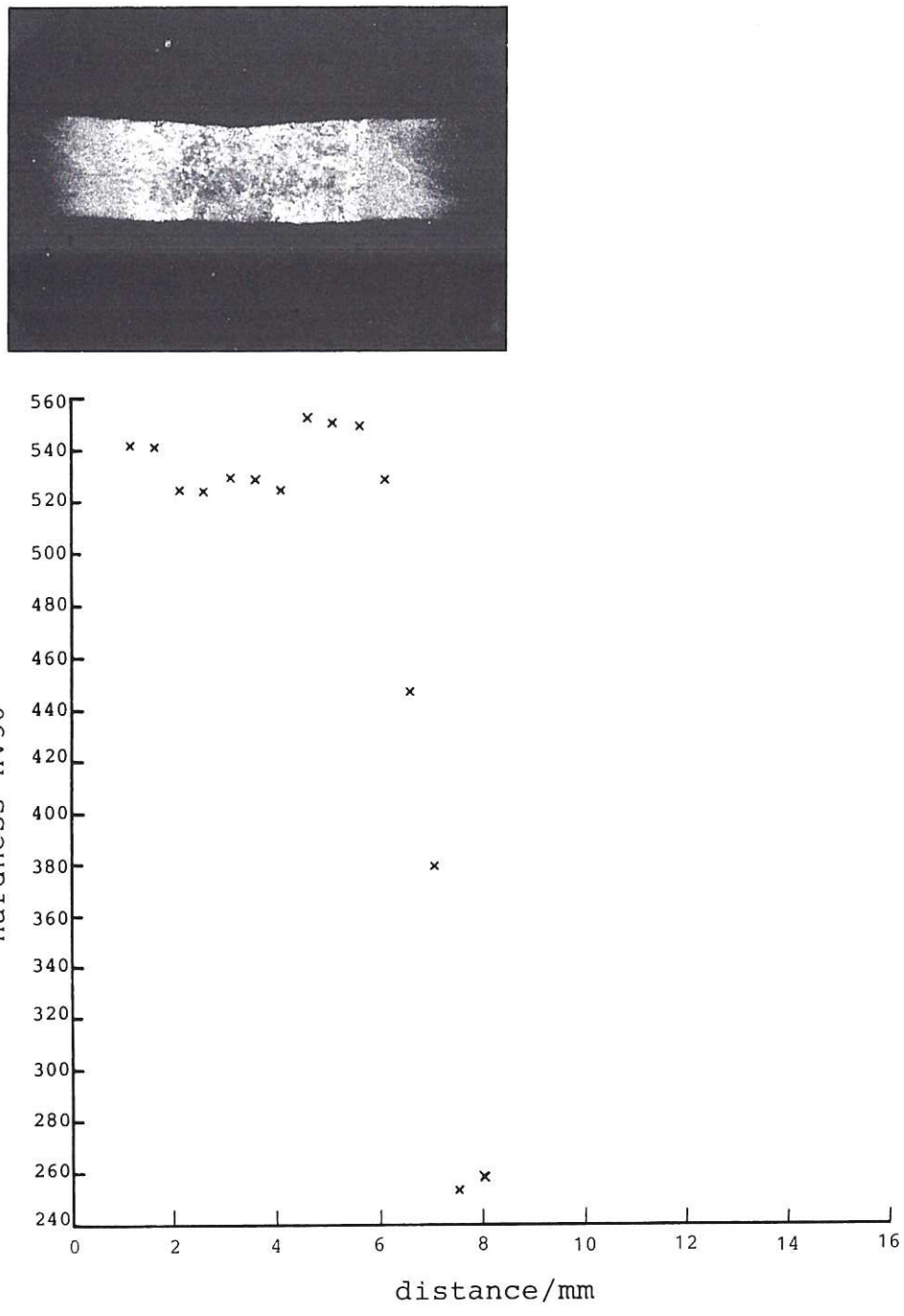

Fig.2 Hardness profile and macrophotograph of 2 mm thick LA7 strip without post-weld heat treatment

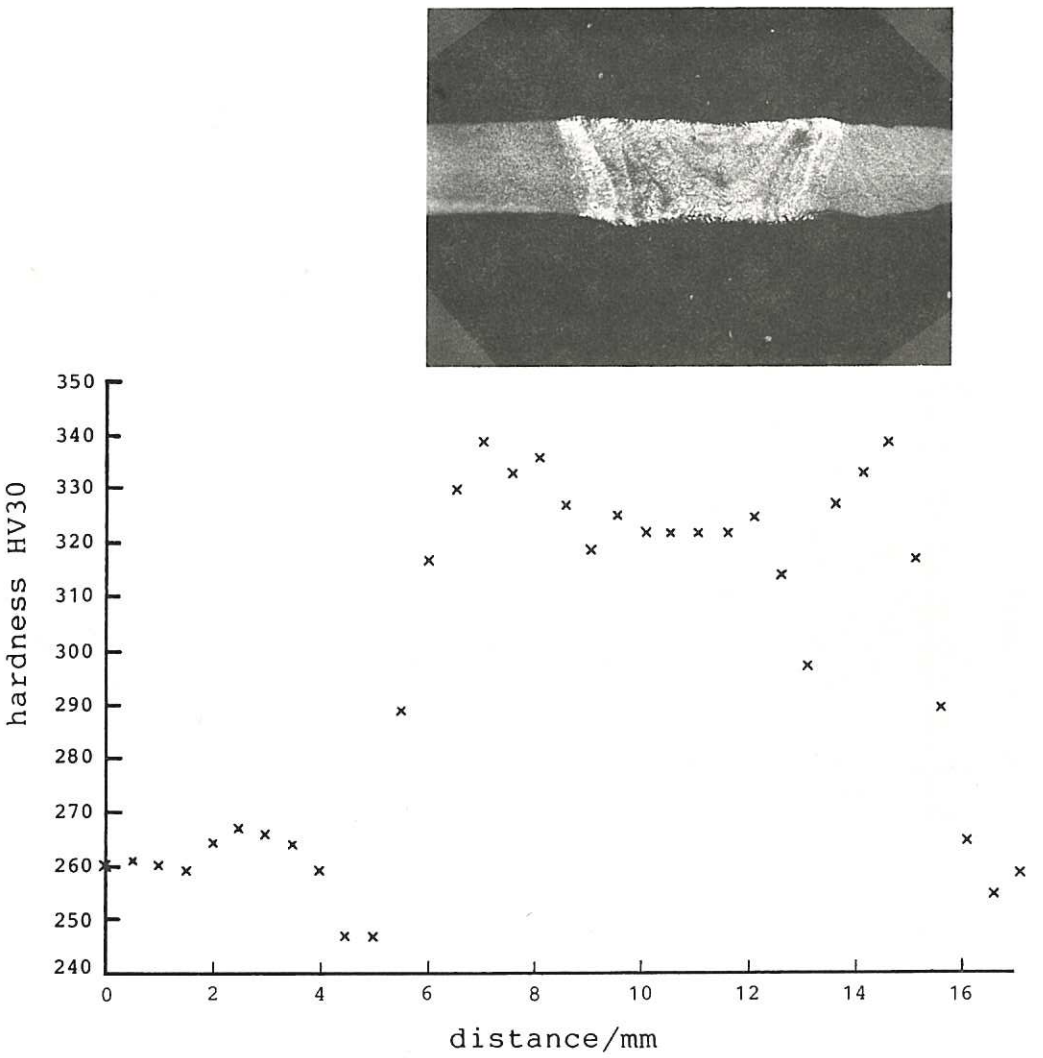

Fig.3 Hardness profile and macrophotograph of 2 mm thick LA7 strip after post-weld heat treatment

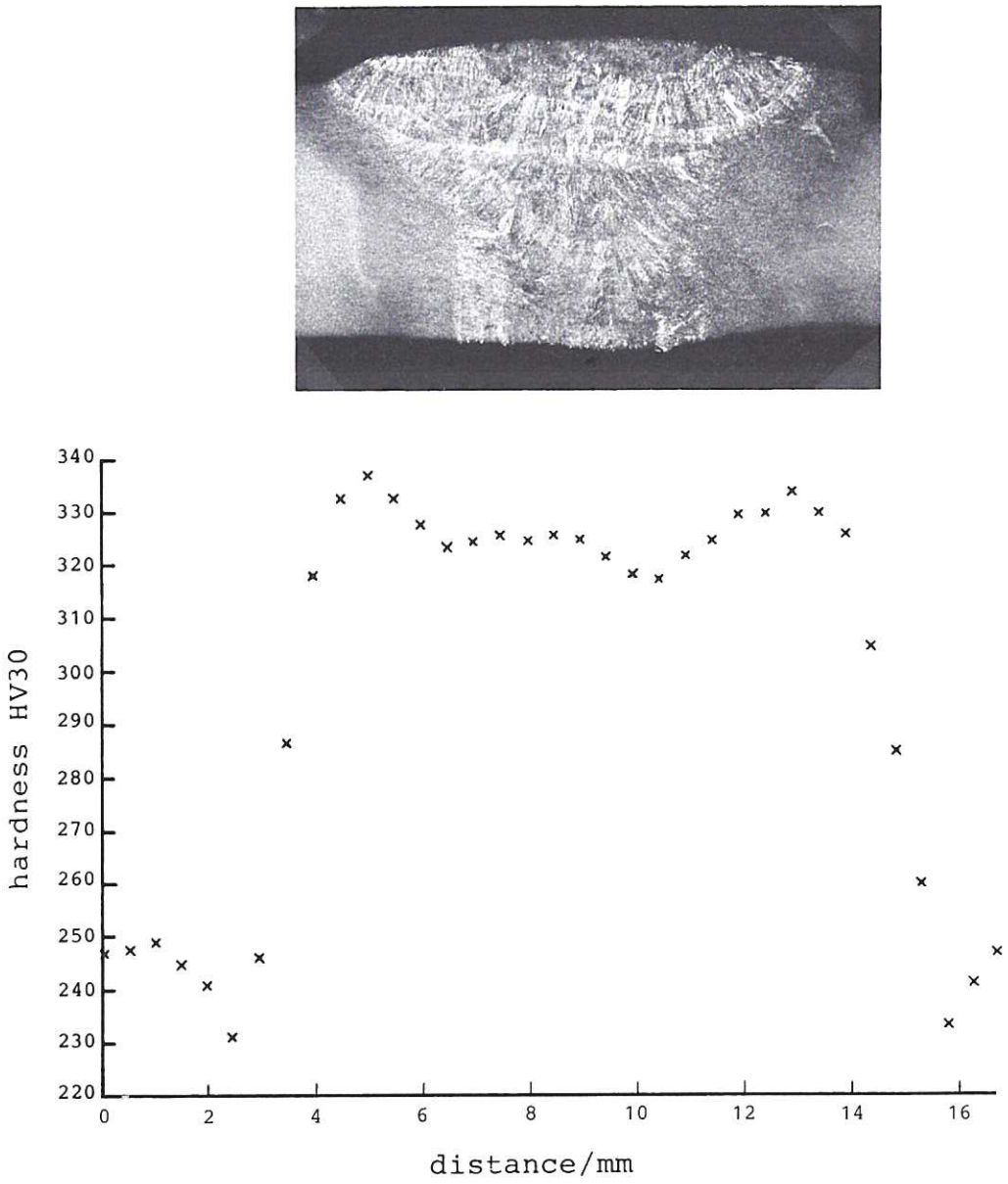

Fig.4 Hardness profile and macrophotograph of 5 mm thick LA7 strip after post-weld heat treatment

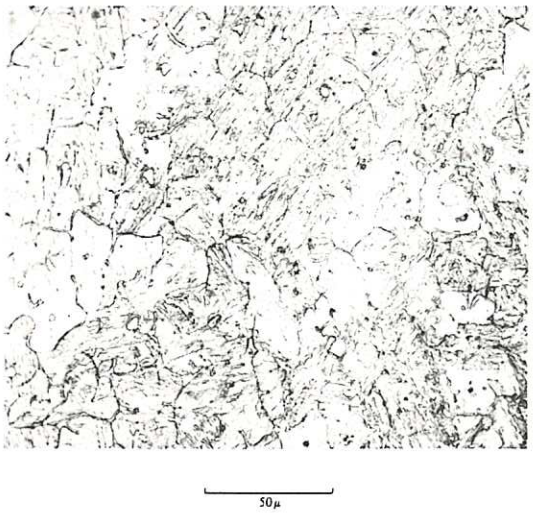

(a) 2 mm strip weld
no post-weld heat treatment

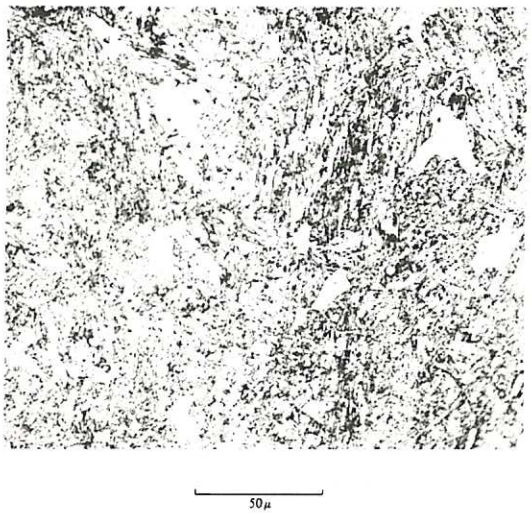

(b) 2 mm strip weld
after post-weld heat treatment

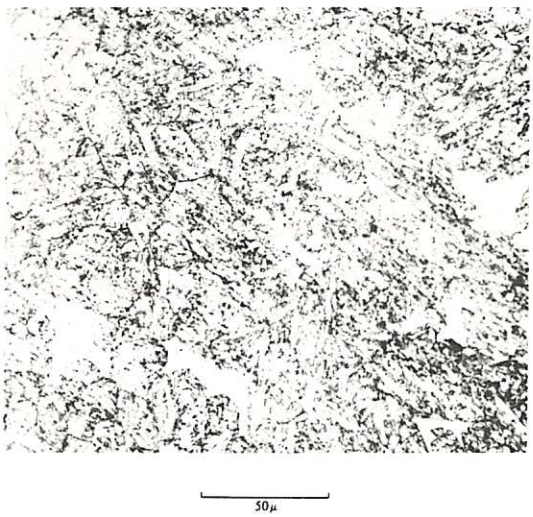

(c) 5 mm strip weld
after post-weld heat treatment

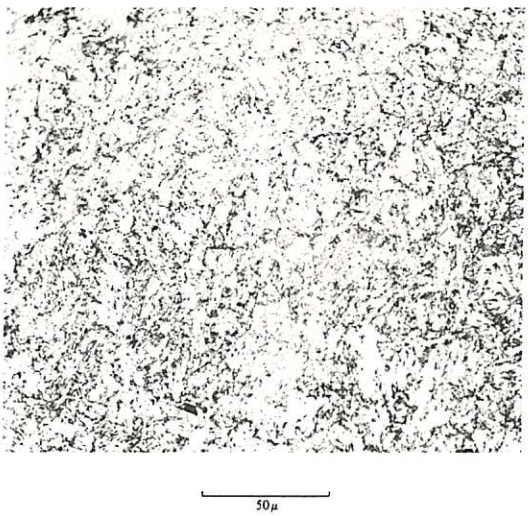

(d) 5 mm strip parent metal
after post-weld heat treatment

Fig.5 Microstructures of welded LA7 strip

relevance, so that relatively short-term tests lasting up to 20,000h provide information sufficient for potential applications. The operating temperatures of first wall and blanket structures are as yet undefined. If reactor operation were to be based on structure temperatures below 400°C then the conventional design procedures would be based on the elevated temperature tensile properties, rather than the creep properties, of the material. For HTR applications, martensitic stainless steels are considered to have limited creep strength above 600°C. It was accordingly thought appropriate to conduct the initial programme of tests in the temperature range 500°-575°C. A range of stresses was selected to give rupture lives up to a maximum of about 10,000h, allowing indications of performance to be obtained by extrapolation to around 20,000h.

The current test programme is incomplete and may run for a further 5000h. The main interest lies in the relative ductility levels, creep strain rates and resulting microstructures after the longer exposures. Nevertheless, the present report provides an interim account of the progress of creep testing.

3.1 Experimental programme

The materials tested are all from the original experimental programme, as listed in Table 1, and comprise the experimental FV448 composition designated Steel 1 and the 9% and 11%Cr, 0.25%V, 3.0%W casts referred to as steels LA7 and LA13. All three materials were heat treated as 19mm bars, following the same procedure as employed earlier [1]. Steel 1 was austenitised for 1h at 1150°C and LA7 and LA13 for 1h at 1100°C. After air cooling, all the steels were tempered for 2h at 675°C.

The creep tests were conducted in UNISTEEL constant load multispecimen, multistring machines in a stagnant air atmosphere and with individual extensometers fitted to each test piece of 24mm gauge length and 7.6mm diameter. The stress-temperature programme is shown in Table 4, which gives the status of the tests at 12 September 1986.

Table 4

Summary of creep tests as at 12.9.86

Temperature °C	Stress MPa	890 N (LA7)			895 N (LA13)			928 N (448)		
		time h	el. %	RA %	time h	el. %	RA %	time h	el. %	RA %
500	540	117	31	71	45	28	66	415	24	64
	510	520	26	66	480	23	58	1980	21	58
	494	1006	26	62	2439	18	42	3600 UB	–	–
	463	5276 UB	–	–	5276 UB	–	–	5276 UB	–	–
550	370	4468	16	49	4263	19	44	3880	12	14
	355	2086 UB	–	–	2086 UB	–	–	2086 UB	–	–
	309	8653 UB	–	–	8653 UB	–	–	8653 UB	–	–
575	324	1290	16	46	1587	17	41	1480	15	50
	278	4013 UB	–	–	4013 UB	–	–	3969	22	57

UB represents an unbroken specimen

CR 87.28/4

3.2 Experimental results

The durations and ductility values for the specimens that have failed to date are presented in Table 4. The rupture lives are shown in the isothermal plots of stress versus rupture life for the three test temperatures in Figs.6-8. In these figures the arrows indicate unbroken test pieces on which tests are continuing and the solid lines represent a fit to data available at Swinden Laboratories for an FV448 type composition. Creep strain values for the low stress tests are shown in Figs.9-12, which give the total plastic strain, in percentage units, as a function of time for each test temperature.

The graphs of rupture life indicate that at 500°C the FV448 type composition is exhibiting a higher rupture strength after short durations, up to 3000h. The relative behaviour of the casts at 550°C after 7000h remains to be established. The elongation value observed for the FV448 composition under a stress of 370MPa is anomalous and requires further investigation. Again, it is too early to discern any differences at 575°C between the three steels.

The creep strain data show that both of the tungsten steels exhibit higher strain rates than the FV448 material under a constant nominal stress at all temperatures. The LA7 steel has a consistently higher creep strain rate than the lower chromium equivalent steel LA13, though the difference at 575°C is not significant.

3.3 Discussion of creep results

The observations so far indicate a clear advantage of the FV448 alloy over LA7 and LA13 in terms of creep resistance at 500°C, though at 550°C and 575°C the difference in respect of rupture life is not significant, despite the lower secondary creep rate for the FV448 steel. The relative difference in creep rates between the 9%Cr and 11%Cr low-activation steels may be appreciable but remains to be established by the results of tests still in progress and by subsequent metallographic examination.

There is some indication that the ductility of the 11%Cr low-activation steel is slightly lower in the rupture tests at 500°C. Further comment will be made when the programme is complete and selected test pieces have been examined metallographically.

4. THE MECHANICAL PROPERTIES OF SELECTED LOW-ACTIVATION STEELS AFTER TEMPERING AT 750°C

The initial study [1] was concerned with the identification of low-activation compositions that would match the properties of the FV448 steel in the high strength condition. Thus the basic mechanical properties of selected experimental compositions were established after hardening and tempering at 675°C. The latter temperature is relatively low for the treatment of martensitic steels for use at elevated temperatures. Whilst a high strength material may have advantages in a fusion reactor structure,

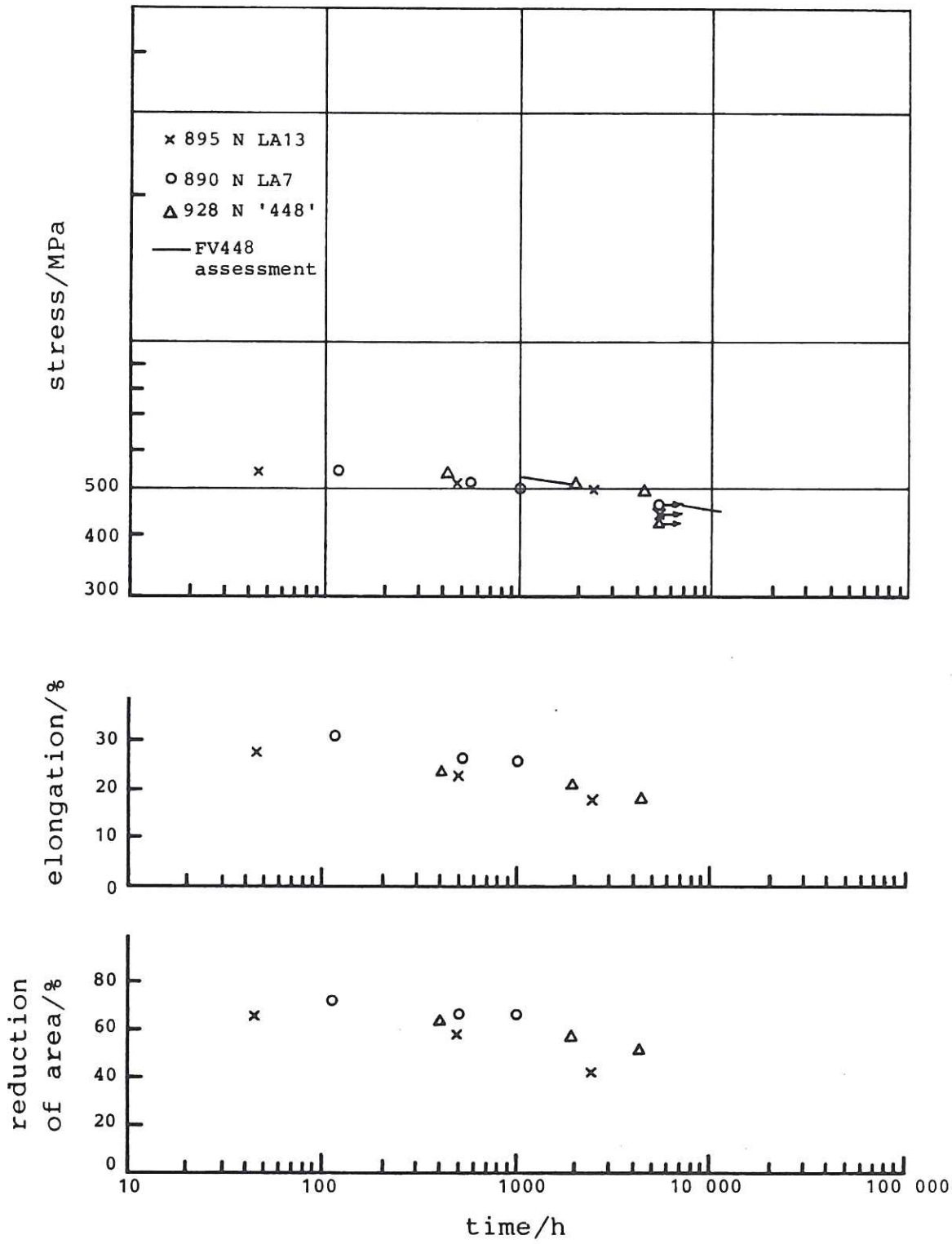

Fig.6 Stress rupture data for martensitic stainless steels tested at 500°C

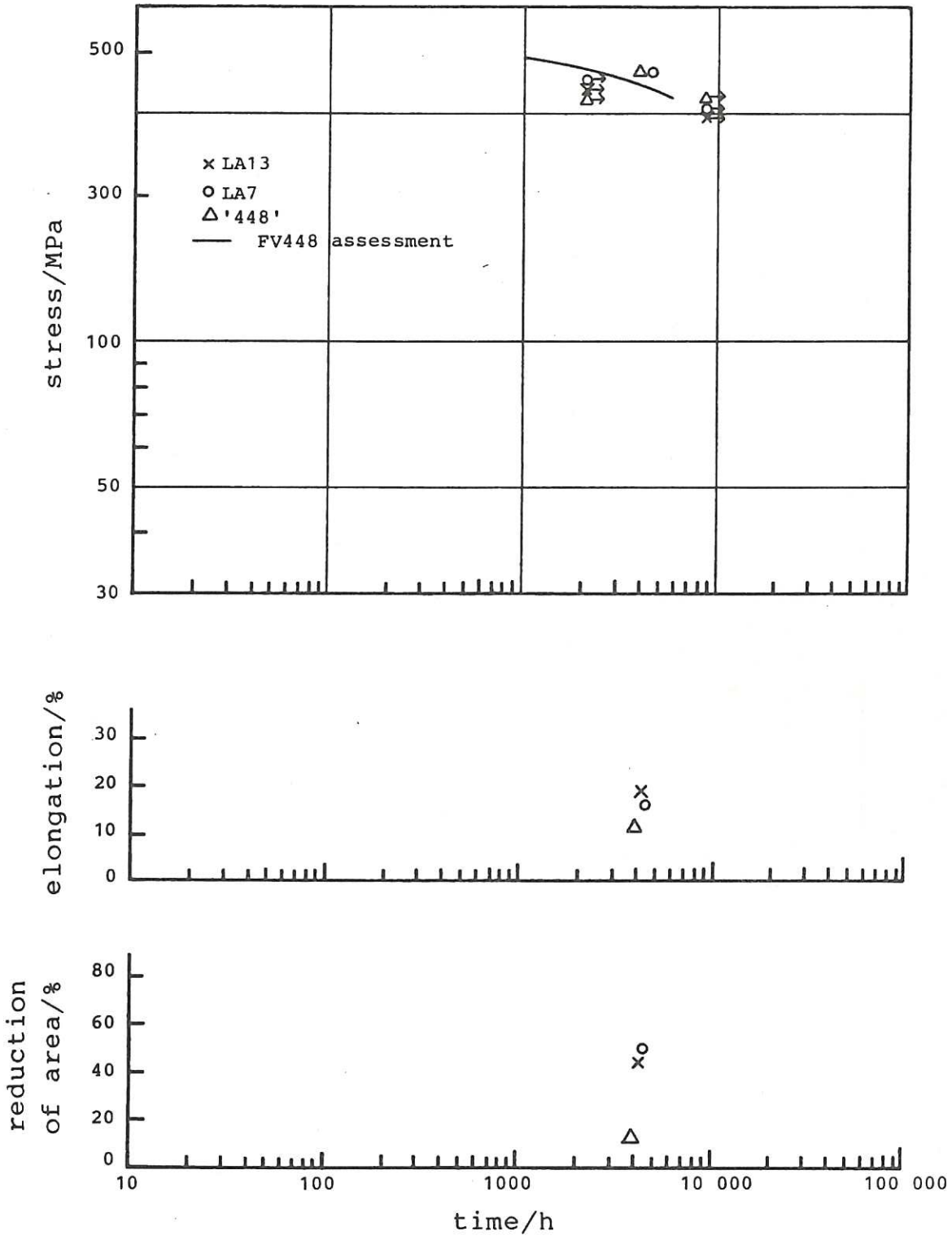

Fig.7 Stress rupture data for martensitic stainless steels tested at 550°C

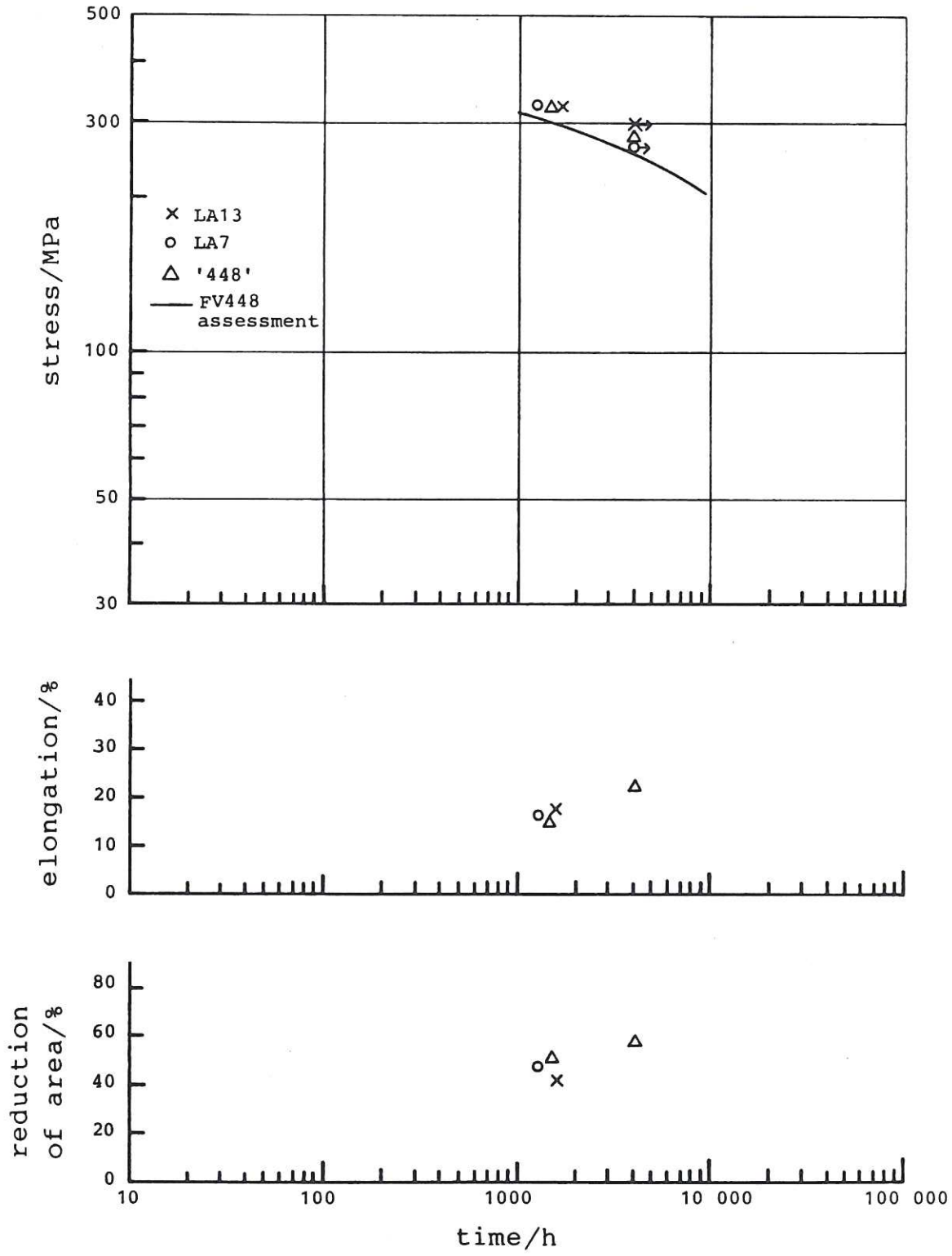

Fig.8 Stress rupture data for martensitic stainless steels tested at 575°C

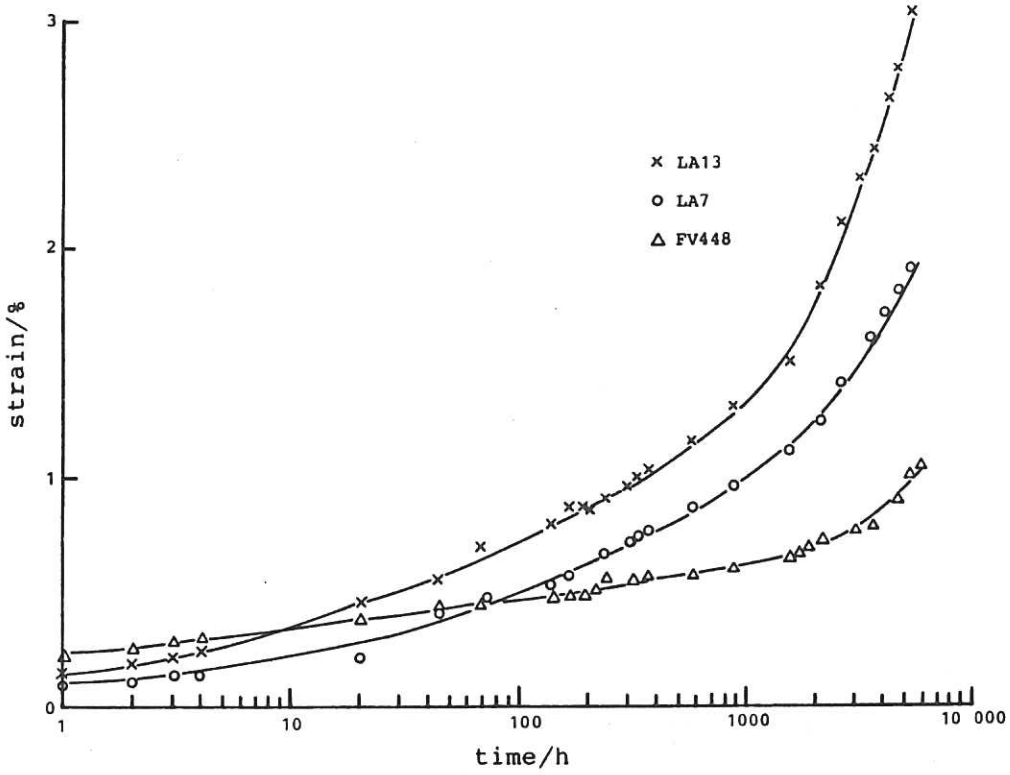

Fig.9 Creep strain curves for martensitic stainless steels at 500°C and 463 MPa stress

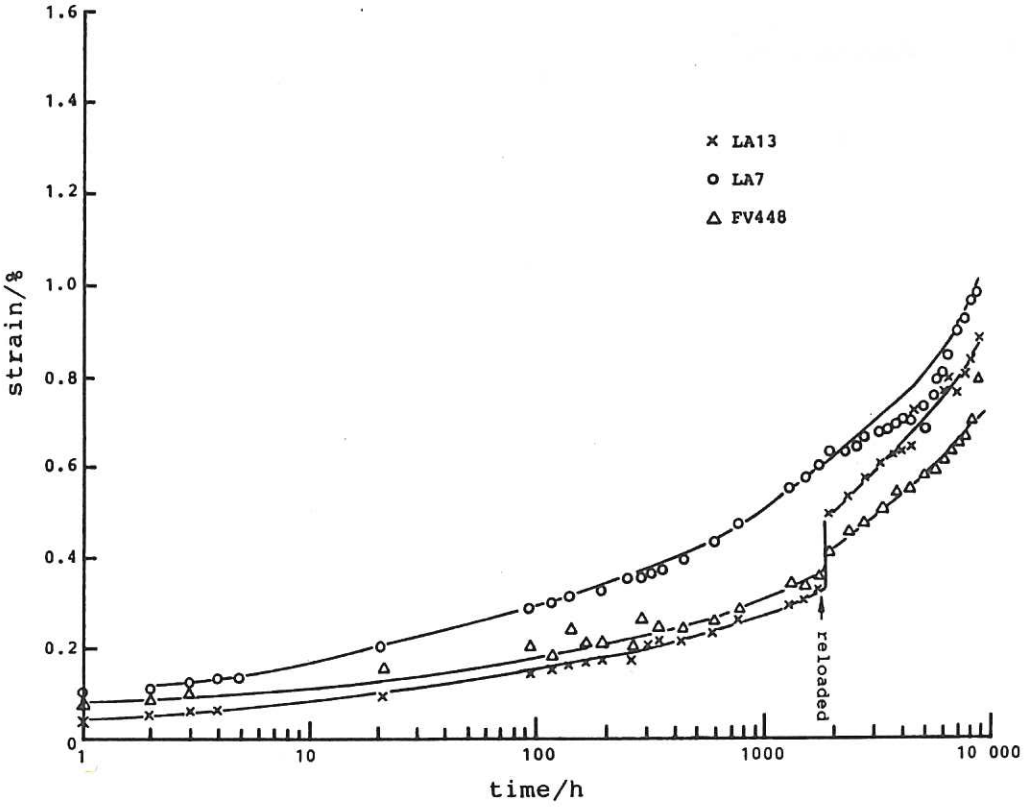

Fig.10 Creep strain curves for martensitic stainless steels at 550°C and 309 MPa stress

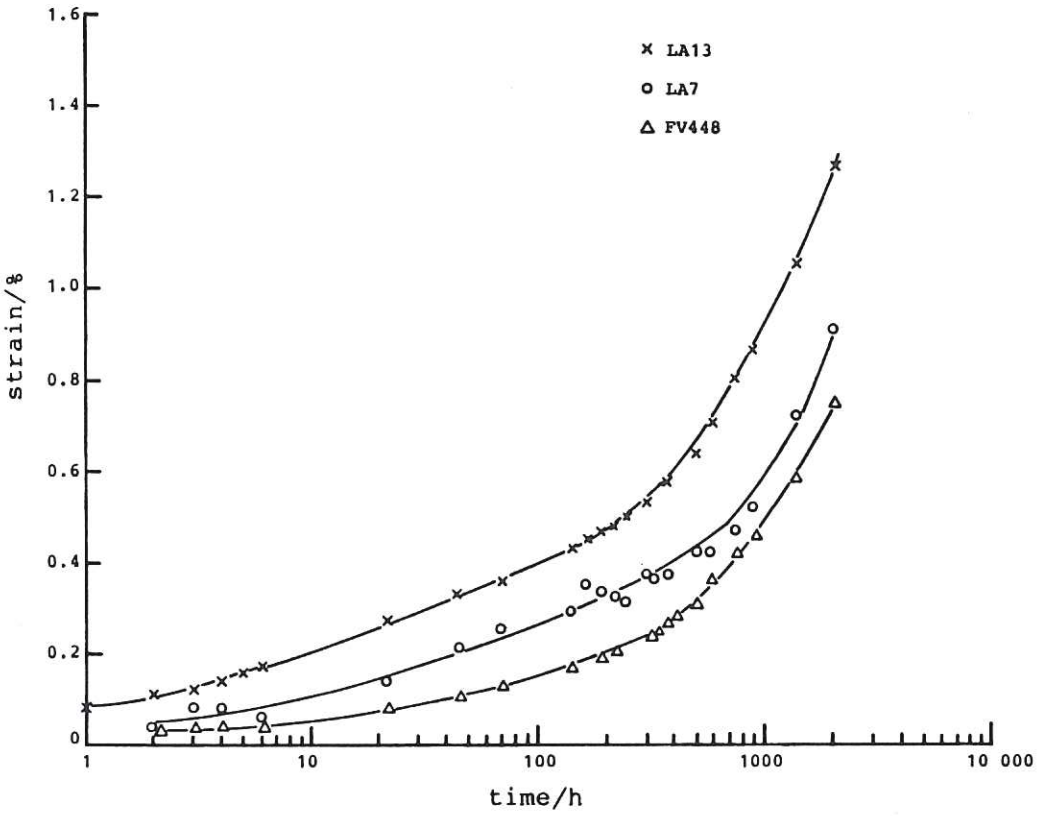

Fig.11 Creep strain curves for martensitic stainless steels at 550°C and 370 MPa stress

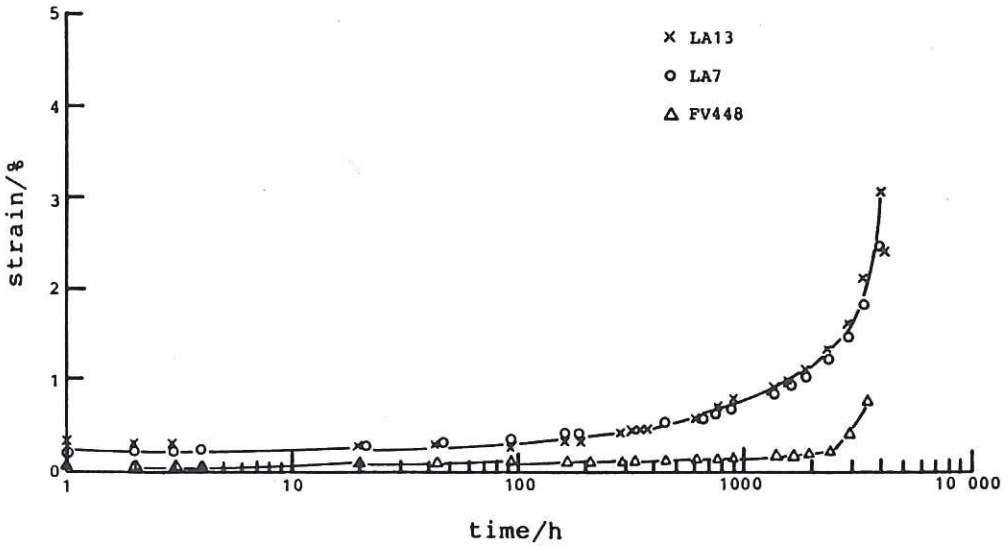

Fig.12 Creep strain curves for martensitic stainless steels at 575°C and 278 MPa stress

for example in reducing the volume of structural material present, it is necessary to take cognisance of the relatively low values of toughness in the high strength condition, especially in view of the upward shift in the ductile-to-brittle transition temperature that is likely to result from radiation-induced embrittlement.

Previous experience with HTR materials has indicated the beneficial influence on toughness to be gained from the use of relatively high tempering temperatures and it was considered appropriate to establish the strength and conventional toughness levels that could be obtained in the low-activation steels by tempering at 750°C. Since an increase in tempering temperature for enhancement of the toughness would imply the acceptance of lower target strength levels, it was thought useful to re-examine the compositions with lower tungsten contents, which showed lower strengths but which would be less susceptible than the 3%W steels to deterioration arising from the longer term precipitation of tungsten-bearing phases. Since these compositions had been screened out in the initial study it was necessary to establish their properties after tempering at 675°C in order to provide a basis for comparison with the higher tungsten steels. The alloys chosen for further study all contained nominally 0.7%W, with 0.25%V (Steel LA4), 0.5%V (Steel LA8) and 0.25%V with 9%Cr (Steel LA12).

4.1 Experimental procedures

The test material comprised 19mm bar from the earlier study, austenitised at 1100°C. After hardening, the bars were tempered for 2h at 750°C or 2h at 675°C, as required. Tensile tests were performed at room temperature and at 450°, 550° and 650°C, and impact transition curves were established using 10mm Charpy and 2mm V-notch test pieces.

4.2 Experimental results

The mechanical properties measured at room temperature are shown in Table 5, which also includes the results obtained earlier for LA7 on tempering at 675°C. The temperature dependence of the elevated temperature 0.2% proof stress is shown in Table 6 and Figs.13-15. On the latter plots, the results obtained by Anderko et al [2] for a low-nitrogen 1.4914 composition are included for comparison. To provide a further indication of the strength of other materials Fig.16 shows the elevated temperature proof strengths as a function of test temperature for four commercial martensitic steels, together with the range reported for the effect of increasing nitrogen content in the 1.4914 steel [2]. The individual impact toughness transition curves for the four steels are given in Figs.17-26.

The room temperature test results are summarised in Fig.27, which shows the relationship between the 0.2% proof strength and the fracture appearance transition temperature (FATT). The effects of exposure at 500°C after tempering at 675°C on the toughness of the 0.7%W steels are summarised in Table 7. All of the compositions exhibited some embrittlement and the effect was relatively highest for LA7, which also had the highest initial FATT value.

Table 5

Mechanical properties of selected steels after tempering for 2h at 675°C and 750°C and for 500h at 500°C and 675°C

Steel no.	Heat Treatment 1h at 1100°C AC +	Impact Charpy 50% brittle	Toughness 2mm V-notch room temperature impact J	Tensile Properties				
				0.1% PS MPa	0.2% PS MPa	UTS MPa	elongation %	RA %
LA4	2h at 675°C	63	20	761	794	947	17	53
	2h at 675°C + 500h at 500°C	93	14	768	802	951	17	50
	500h at 675°C	3	105	512	534	712	22	64
	2h at 750°C	6	108	543	567	751	21	62
LA8	2h at 675°C	53	19	779	814	967	14	50
	2h at 675°C + 500h at 500°C	76	16	781	816	967	17	54
	500h at 675°C	−3	153	482	503	702	24	64
	2h at 750°C	−7	140	496	519	731	24	66
LA12	2h at 675°C	56	22	758	796	955	15	50
	2h at 675°C + 500h at 500°C	77	21	775	809	944	16	55
	500h at 675°C	−8	142	477	497	670	24	66
	2h at 750°C	5	117	514	535	713	24	66
LA7	2h at 675°C	44	22	801	838	1022	14	58
	2h at 750°C	15	60	595	622	837	20	54

CR87.28/5

4.3 Discussion of tensile properties

Table 6 and Fig.27 show the loss in strength for the four steels on tempering at 750°C, rather than 675°C, with the associated beneficial effects of tempering at 750°C on the impact transition temperature. It is seen that, although the overageing treatment of 500h at 675°C gives a higher value of the tempering parameter, its employment results in a less favourable combination of proof stress and FATT for LA7 steel. In the case of the steels with lower tungsten contents, however, the more intense tempering treatment, in parametric terms, led to slightly lower strengths with similar toughnesses.

Steels LA4 and LA12 were closely matched in composition, apart from the difference in chromium content. As was found with steels LA7 and LA13 on tempering at 675°C, the 11%Cr steel was slightly stronger at room temperature. It is interesting to note, however, that the reduction in chromium content appears to confer a small advantage in elevated temperature strength at 550°C. This observation is consistent with the

Table 6

Elevated temperature tensile properties of selected steels after hardening and tempering at 675°C and 750°C

Steel	Tempering temperature °C	Test temperature °C	0.1% PS MPa	0.2% PS MPa	UTS MPa	elongation %	RA %
LA4	675	450	594	625	721	14	60
		550	437	461	569	20	75
		650	286	308	420	24	82
LA4	750	450	407	433	552	16	62
		550	325	342	432	14	82
		650	177	185	288	32	92
LA8	675	450	610	643	745	14	55
		550	466	494	617	17	66
		650	245	271	401	25	80
LA8	750	450	392	419	537	19	70
		550	314	330	423	23	78
		650	157	168	280	30	88
LA12	675	450	584	615	715	14	61
		550	442	467	547	20	72
		650	273	294	412	23	78
LA12	750	450	411	438	540	16	67
		550	329	349	432	22	80
		650	172	183	286	31	91

CR87.28/6

apparent effect of chromium content on the creep strain rate noted for LA7 and LA13 (see section 3 above) but not with the earlier results which indicated that, for the 3%W steels, the room and elevated temperature proof strengths of the 11%Cr steel were superior at temperatures above 450°C.

The present results for steels LA4 and LA8 indicate no advantage from increasing the vanadium concentration from 0.25% to 0.46%. This finding confirms the trend observed in the initial study, which showed that this increase was effective only for temperatures below 675°C.

The results indicate that a steel of the LA12 type, containing 9%Cr, 0.25%V and 0.6%W, is capable of giving room temperature and 550°C proof stress values above 500 and 300MPa, respectively, combined with a subzero-Charpy FATT. Table 8 represents an attempt to put these strength values into perspective. The table summarises typical room and elevated

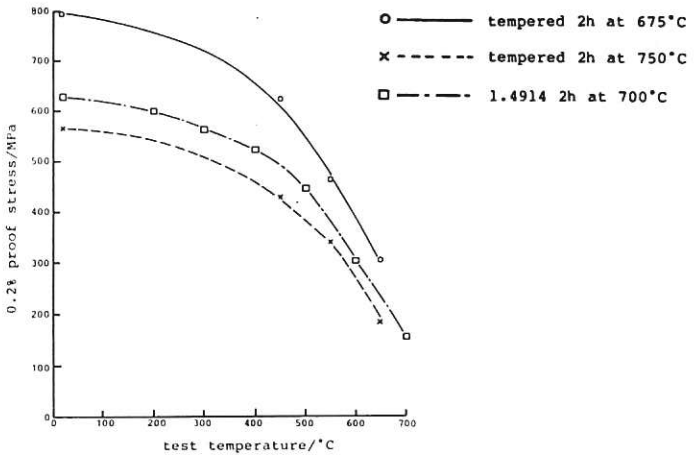

Fig.13 Graph showing the effect of test temperature on the 0.2% proof stress of LA4 after hardening and tempering at 675°C or 750°C in comparison with modified DIN 1.4914 steel

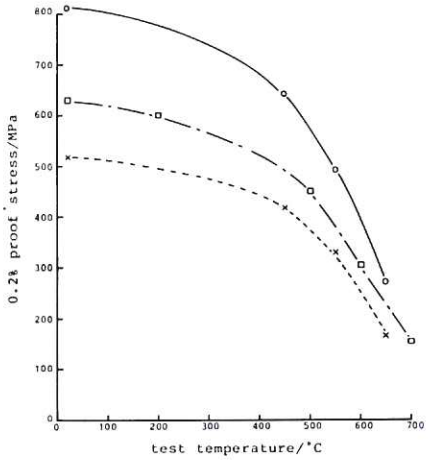

Fig.14 Graph showing the effect of test temperature on the 0.2% proof stress of LA8 after hardening and tempering at 675°C or 750°C in comparison with modified DIN 1.4914 steel

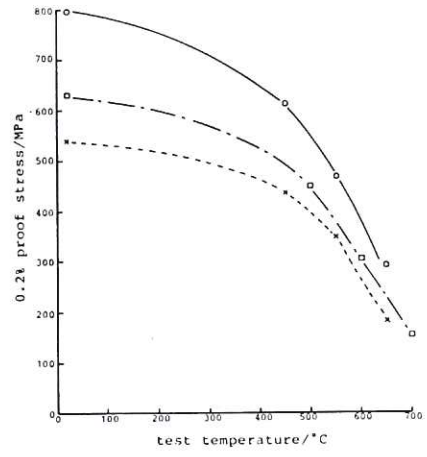

Fig.15 Graph showing the effect of test temperature on the 0.2% proof stress of LA12 after hardening and tempering at 675°C or 750°C in comparison with modified DIN 1.4914 steel

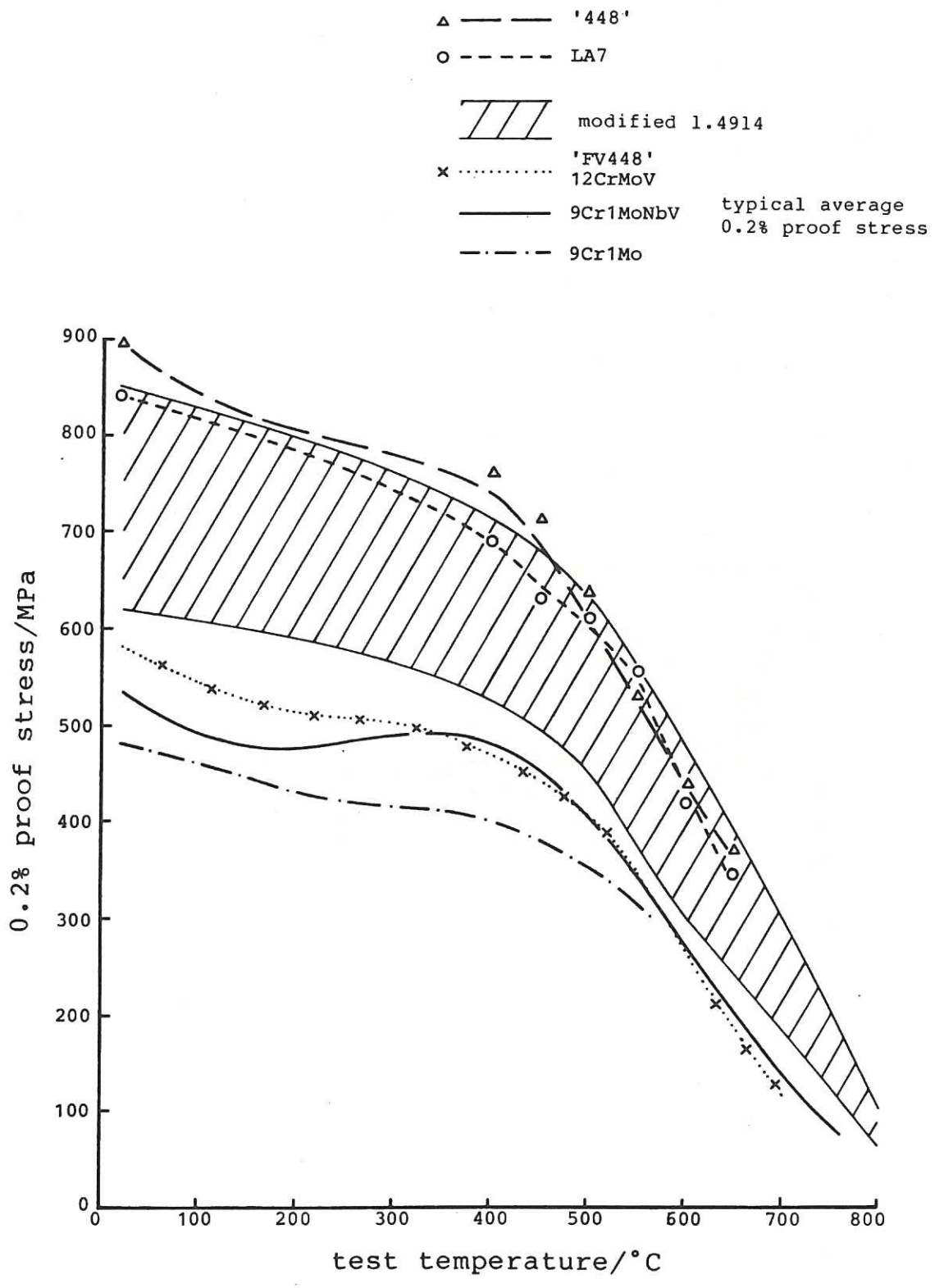

Fig.16 Typical room and elevated temperature 0.2% proof stress values for commercial martensitic stainless steels in comparison with LA7 and modified DIN 1.4914 steel

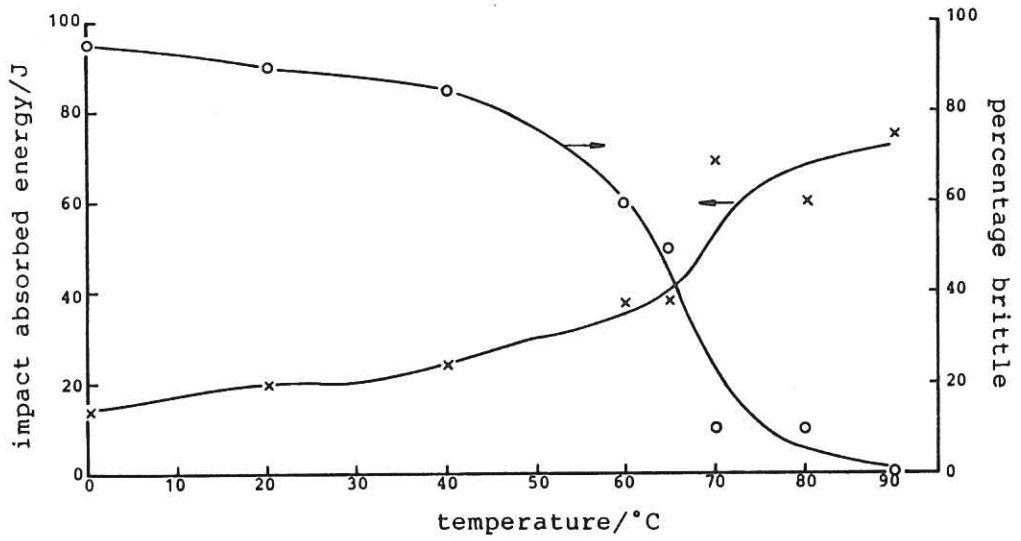

Fig.17 Impact transition temperature data for steel LA4 after 1h at 1100°C and 2h at 675°C

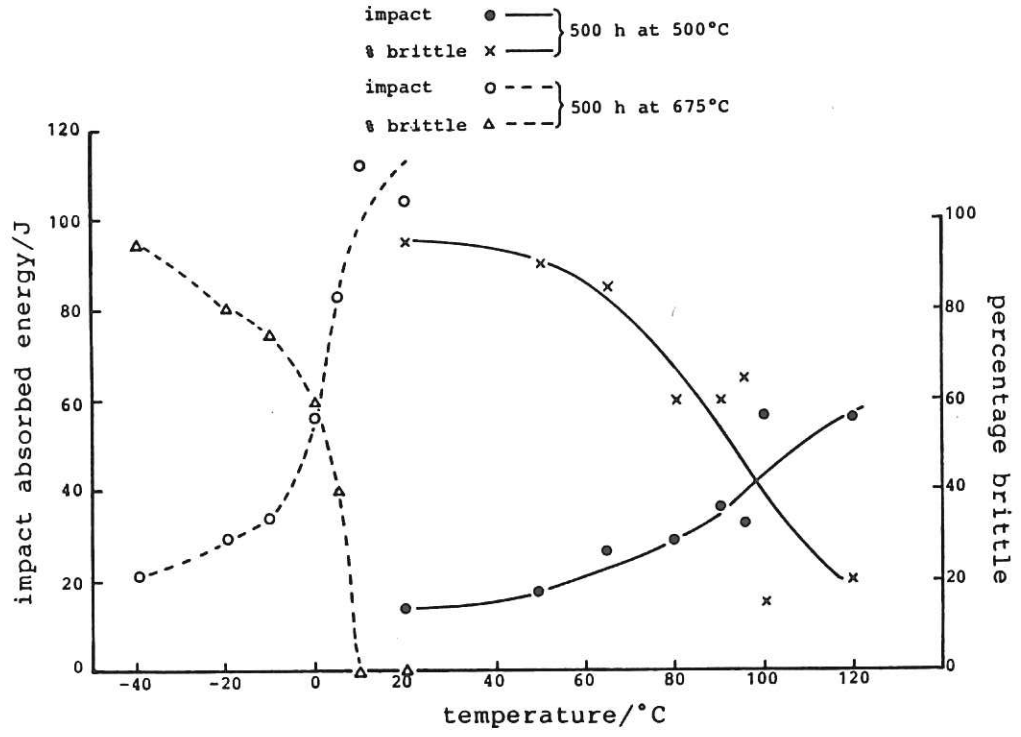

Fig.18 Impact transition temperature data for steel LA4 after 500h tempers

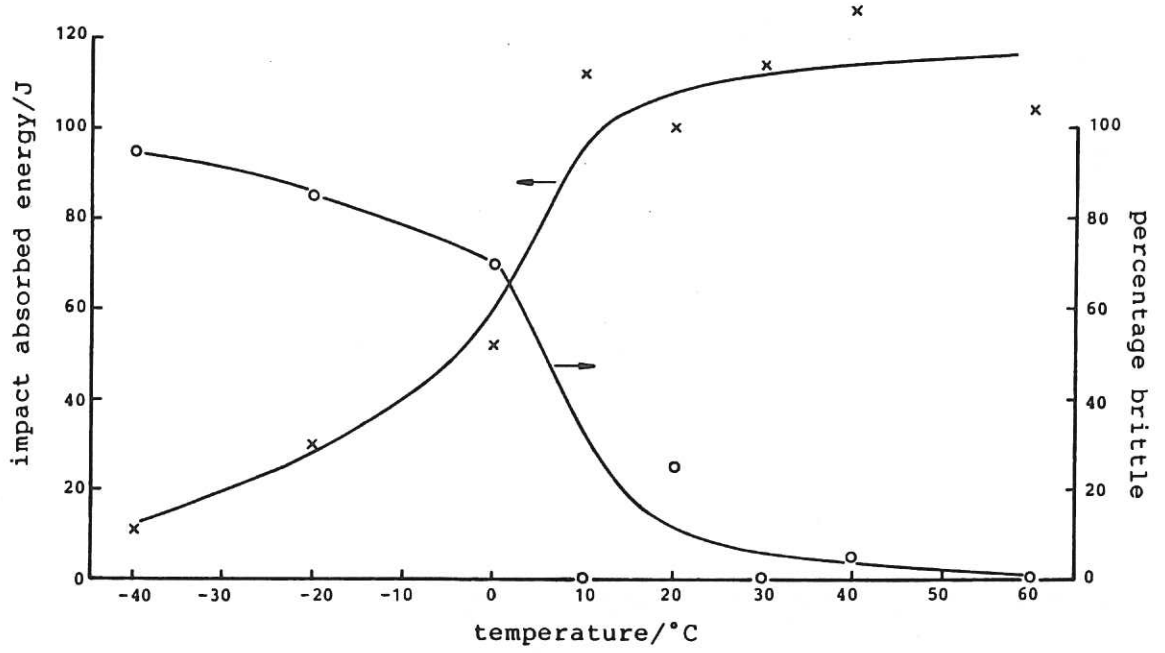

Fig.19 Impact transition temperature data for steel LA4 after 1h at 1100°C and 2h at 750°C

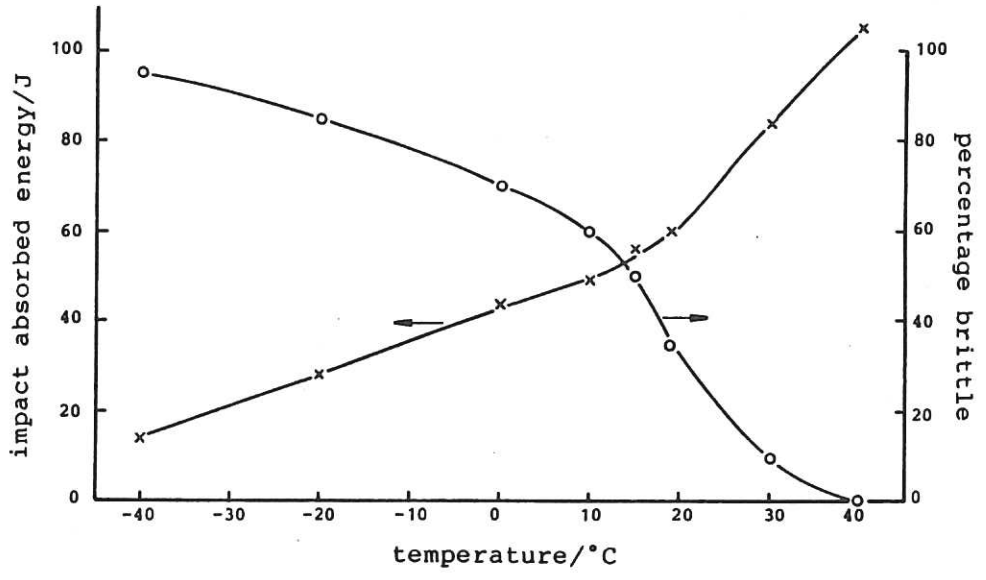

Fig.20 Impact transition temperature data for steel LA7 after 1h at 1100°C and 2h at 750°C

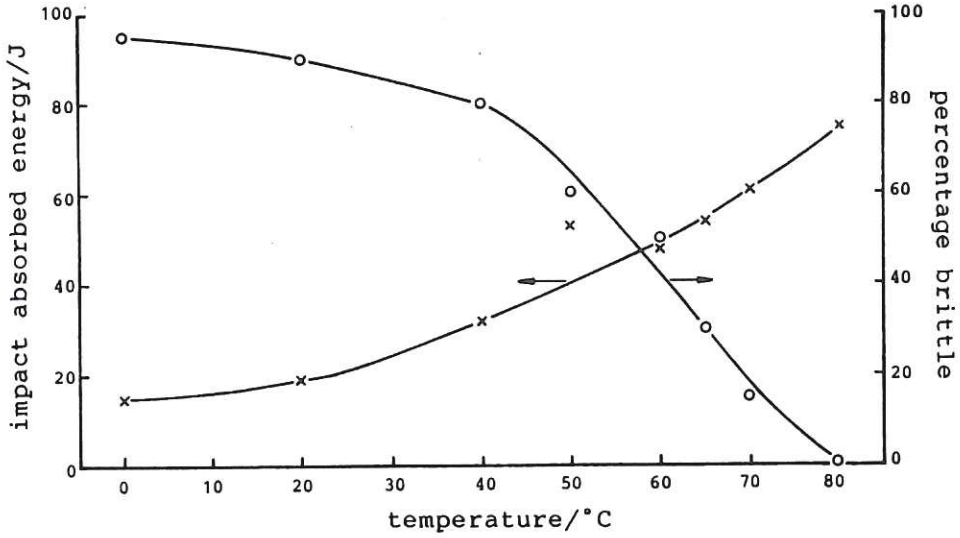

Fig.21 Impact transition temperature data for steel LA8 after 1h at 1100°C and 2h at 675°C

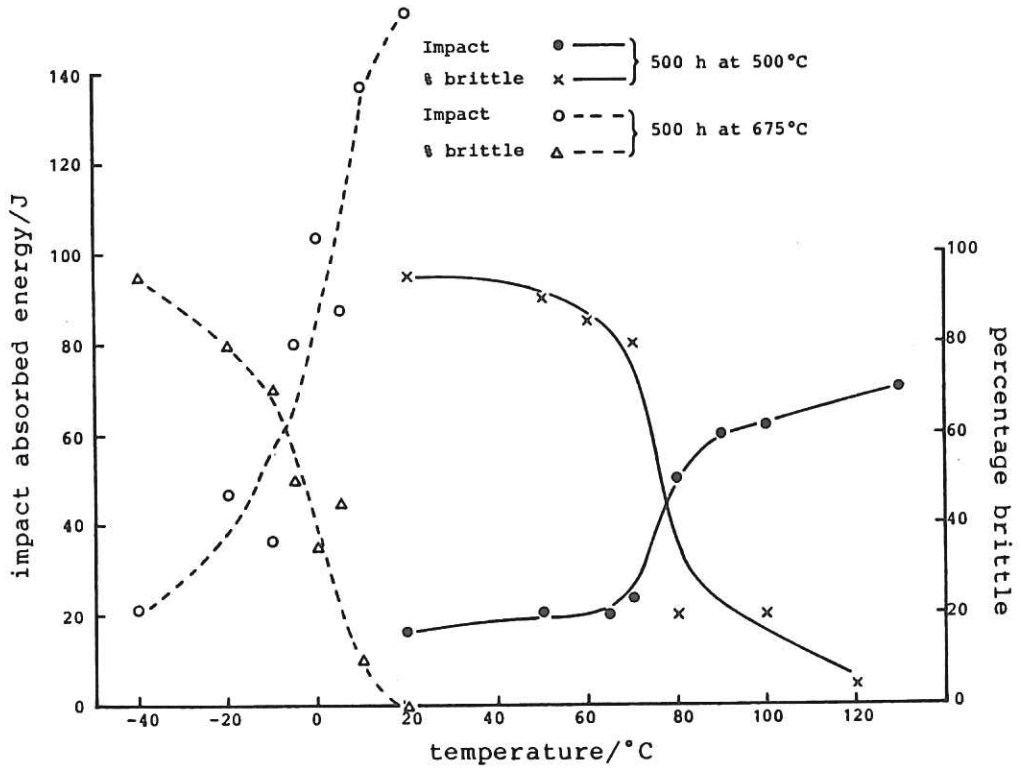

Fig.22 Impact transition temperature data for steel LA8 after 500h tempers

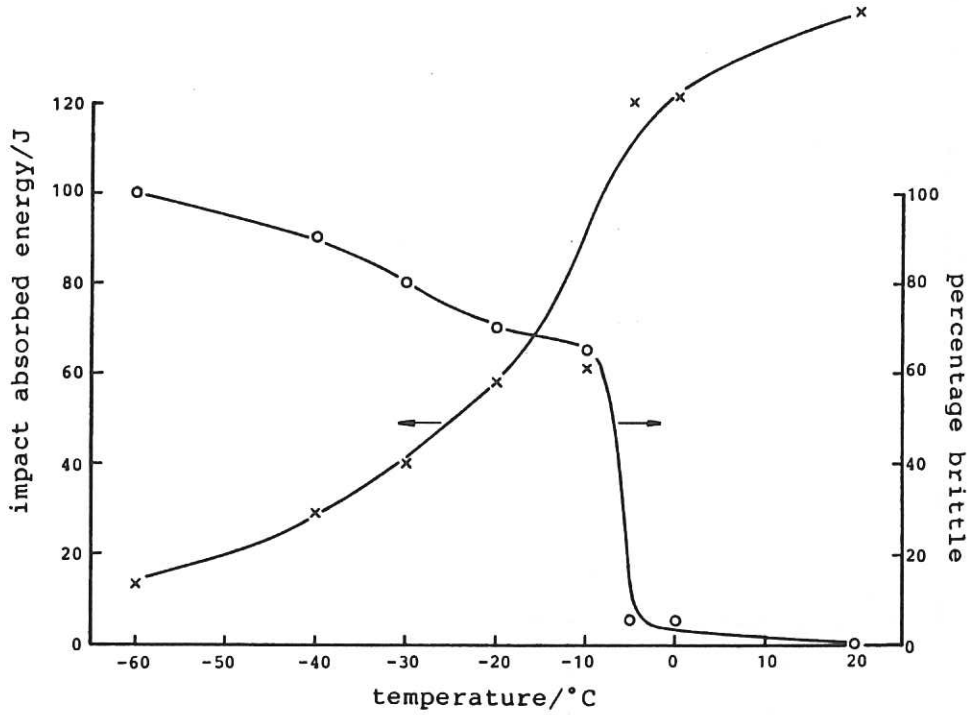

Fig.23 Impact transition temperature data for steel LA8 after 1h at 1100°C and 2h at 750°C

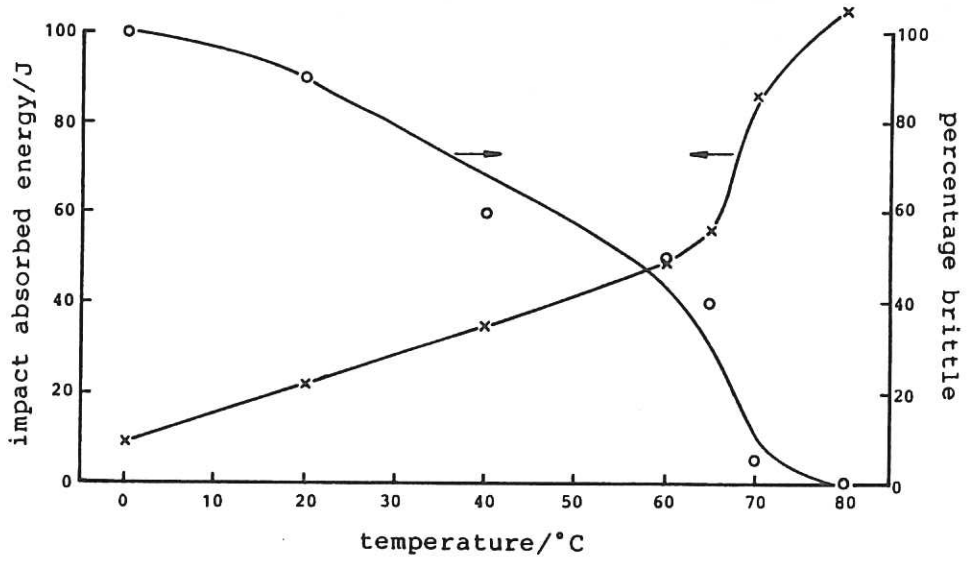

Fig.24 Impact transition temperature data for steel LA12 after 1h at 1100°C and 2h at 675°C

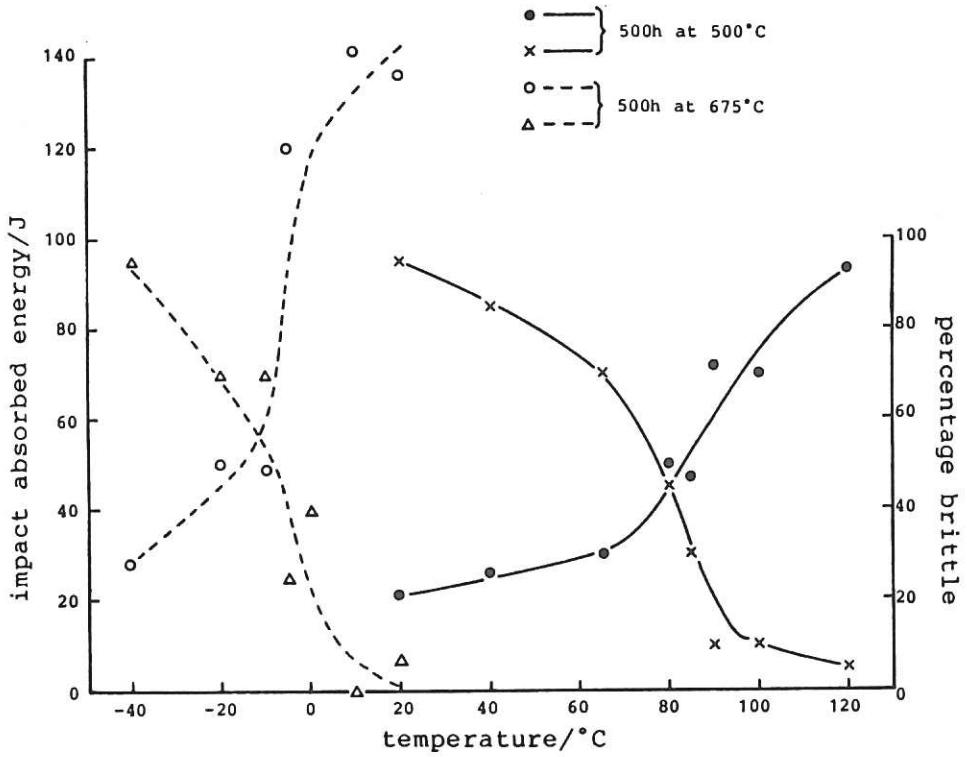

Fig.25 Impact transition temperature data for steel LA12 after 500h tempers

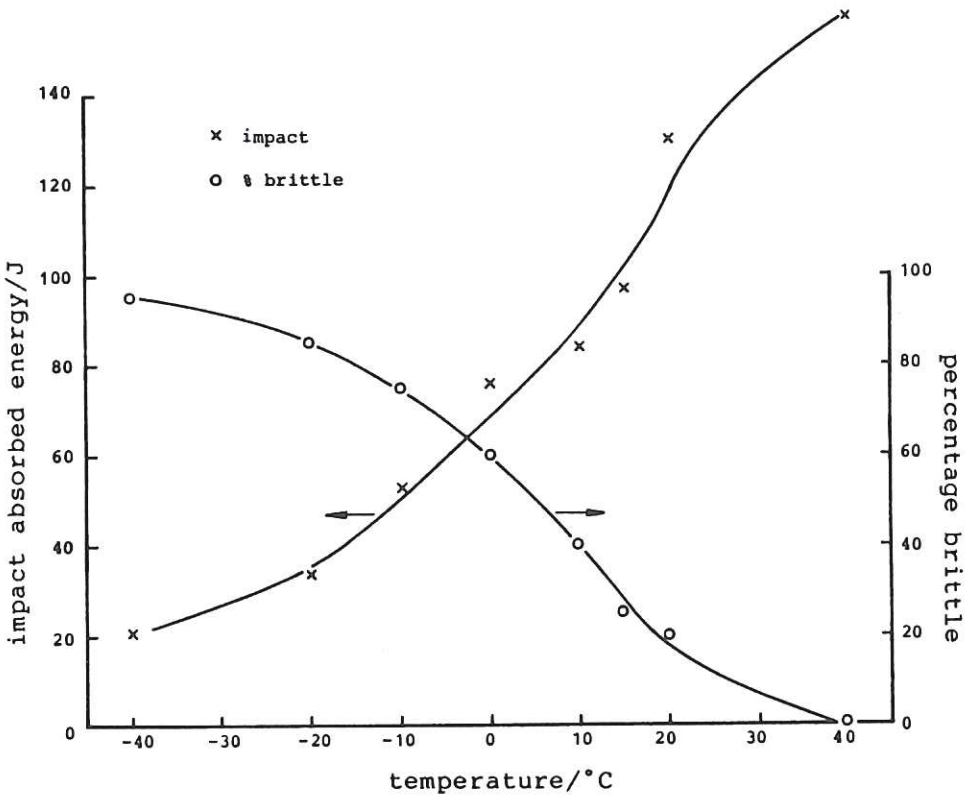

Fig.26 Impact transition temperature data for steel LA12 after 1h at 1100°C and 2h at 750°C

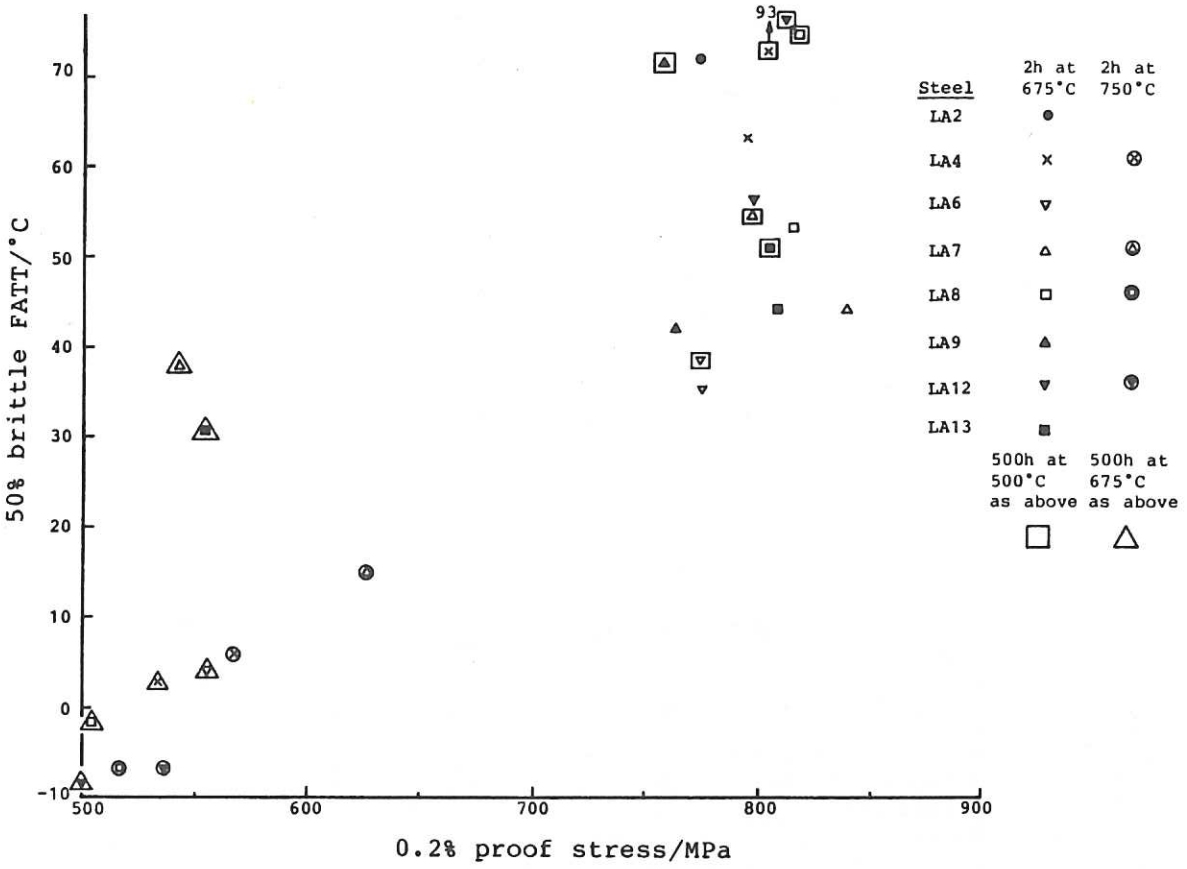

Fig.27 Relationship between fracture appearance transition temperature and 0.2% proof stress of selected steels after optimum heat treatment and overageing

Table 7

Effect of exposure for 500h at 500°C after tempering for 2h at 675°C

Steel	ΔFATT °C	Δ0.2% PS MPa
LA4	+30	+5
LA7	+10	−10
LA8	+20	0
LA12	+20	+15
LA13	+5	0

CR 87.28/7

temperature tensile properties for established martensitic stainless steels and allows them to be compared with selected results from the present programme. It is important to distinguish between the values of properties adopted as standard for a material and from which engineering design stresses on components are derived, and the average property values obtained with production materials. The latter should always be the higher. Taking these latter average values, it is clear that 9% and 11%Cr, 0.25%V, 0.6-1.0%W compositions can attain strength levels comparable with those of current steels when given high temperature tempering treatments.

Table 8

Strength levels of commercial and experimental martensitic stainless steels

Steel		heat treated condition	room and elevated temperatures 0.2% PS (MPa)			
			RT	450°C	550°C	650°C
9Cr-1Mo	design average	980°C/760°C (2h)	400 500	310 390	230 320	
9Cr-MoNbV	design average	1048°C/750°C (2h)	416 520	340 450	260 340	160 200
12Cr-MoV	design average	1050°C/760°C (2h)	470 570	330 440	250 350	
FV448 commercial data		1150°C/675°C (2h)	820	680		
Steel 1		1150°C/675°C (2h) 675°C (500h)	890 627	714	535	373
LA4		1100°C/675°C (2h) 675°C (500h)	794 534	625	461	308
LA6		1100°C/675°C (2h) 675°C (500h)	776 554	625	482	277
LA7		1100°C/675°C (2h) 675°C (500h)	838 570	629	552	340
LA8		1100°C/675°C (2h) 675°C (500h)	814 503	643	494	271
LA9		1150°C/675°C (2h) 675°C (500h)	763 472	593	446	243
LA12		1100°C/675°C (2h) 675°C (500h)	796 497	615	467	294
LA13		1100°C/675°C (2h) 675°C (500h)	804 553	651	495	341

CR87.28/8

Further investigations are required to characterise the microstructures and assess the stability of the phase distributions resulting from high temperature tempering. Any such work must, however, be considered in the

light of further compositional modifications that might be needed for other reasons, in particular to achieve austenite grain refinement (see section 5) and to reduce the nitrogen content (see section 6).

5. AUSTENITE GRAIN SIZE CONTROL IN LOW-ACTIVATION MARTENSITIC STEELS

It was recognised in the initial study that the elimination of niobium, on the grounds on its radioactivation, removed the principal austenite grain refining agent present in the FV448 composition. One consequence of the absence of niobium was evident when the prior austenite grain sizes of the experimental FV448 and low-activation alloys were compared, as summarised in Table 9. The magnitude of the improvements in toughness obtainable through grain refinement in the low-activation steels has not yet been established. Nevertheless, on the assumption that a high level of initial toughness will be required for structural integrity, it was judged essential to examine methods by which grain refinement may be achieved. One such method, already demonstrated in the welding study, involves the

Table 9

Prior austenite grain size (ASTM), delta ferrite content and hardness of the steels as air cooled after austenitising

Steel no.	austenitising temperature °C	grain size ASTM	delta ferrite content %	as-cooled hardness HV30
1	1100	9	0	462
	1150	9 – 9½	0	457
2	1100	4½	0	487
3	1100	5	0	496
4	1100	5	0	504
5	1100	4½	0	497
6	1100	4½	<5	557
7	1100	5	<5	546
8	1100	5	0	500
9	1100	7	0	470
	1150	5	0	498
10	1100	4½ – 5	0	500
11	1100	4½	0	528
12	1100	4½ – 5	0	469
13	1100	5	0	497
commercial FV448	1150	6 – 6½	0	434

CR 87.28/9

use of low austenitising temperatures. The latter obviously limit the opportunity for thermally-activated grain growth, with the additional advantage that any undissolved second phases can also pin grain boundaries against movement. As was apparent in the welding study (see section 1), the penalty for this solution is a drastic loss in strength.

Alternative methods rely on the development of a stable dispersion of particles at the temperatures employed for austenitising. The size range and volume fraction of the particles required for effective boundary pinning can be calculated from theory [3,4]. Broadly, two ways of achieving such dispersions are possible. The first requires inert particles of a suitable size, preferably below 0.5μm, which are added to the liquid steel or formed within it as the result of a reaction, for example as deoxidation products. Because of the difficulties of control this route is little used. The only effective pinning distributions are those found in materials made by powder metallurgy or internal oxidation routes.

Melt-nucleated phases such as oxides and titanium nitride, though capable of contributing to grain boundary pinning, are usually too coarse to be fully effective in reaustenitisation and have deleterious side effects. Practical grain refining additions rely principally on solid state solution and reprecipitation processes, where precipitation occurs at a temperature above that at which reaustenitisation will be effected or where the kinetics of particle dissolution on reheating allow an effective dispersion during austenitising. The choice of such additions for austenitising temperatures above 1000°C is largely confined to nitride-forming elements, and those acceptable in low-activation compositions are tantalum, titanium (up to a maximum of about 0.1% from radiological considerations) and hafnium.

Some solubility product data are available for the above elements in steel, although the product can be affected by the chemical activities of other elements present. Values given in Table 10 [5] show that tantalum is comparable with niobium in its nitride solubility at 1110°-1200°C. Titanium would be expected to be relatively less effective in view of the lower solubility of its nitride. Hafnium is likely to be even less effective and would be difficult to control as a grain refining addition, given its high affinity for oxygen. Accordingly, initial experiments were made to establish the effects of tantalum additions.

The application of a grain refining addition is illustrated schematically for tantalum in Fig.28, which shows the solubility product relationship for TaN in steel at 1110° and 1200°C. For tantalum and nitrogen concentrations below the product curves, both elements are in solid solution at the temperature indicated. The difference between the two lines indicates the volume fraction of TaN that could be dissolved in a high temperature treatment, for example during hot working, prior to austenitising for the purpose of hardening.

Table 10

Equilibrium solubility products of nitrides in solid iron

temperature °C	[%V][%N]	[%Nb][%N]	[%Ta][%N]	[%Ti][%N]	[%Zr][%N]
1300	1.3×10^{-2}	3.1×10^{-3}	8.8×10^{-3}	1.9×10^{-6}	1.6×10^{-6}
1200	5.3×10^{-3}	1.3×10^{-3}	2.5×10^{-3}	4.2×10^{-7}	$<4\times10^{-7}$
1100	2.0×10^{-3}	5.0×10^{-4}	5.7×10^{-4}	$<1.0\times10^{-7}$	–
1000	6.3×10^{-4}	1.6×10^{-4}	1.1×10^{-4}	–	–
900	1.6×10^{-4}	4.4×10^{-5}	1.5×10^{-5}	–	–

CR 87.28/10

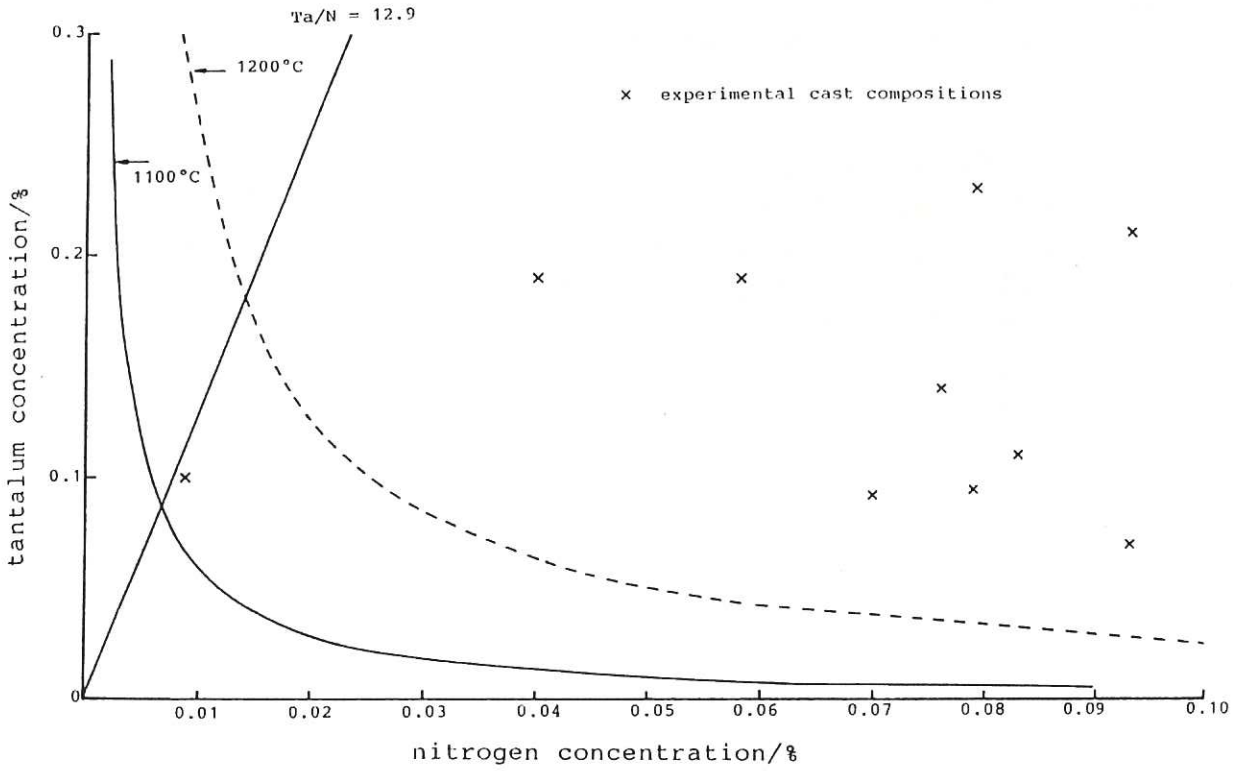

Fig.28 Graph showing the solubility product relationship for TaN in steel at 1100°C and 1200°C

The sequence leading to development of the particles responsible for grain boundary pinning is that, in the final stages of hot working, any undissolved particles will coarsen to form relatively large particles. The dissolved Ta and N at the end of hot working will precipitate as fine particles of TaN on cooling, to an extent that depends on the cooling rate. During reheating for hardening, more precipitation will take place and the

particles will coarsen at the austenitising temperature. It is, however, the finer initial size of the precipitated particles that should make them more effective as boundary pinning agents than the coarser, undissolved particles. It follows that the amount of precipitate that can be taken into solution between the hot working and austenitising temperatures is an important factor in grain size control.

The maximum volume fraction of precipitate would be obtained if Ta and N were present in the stoichiometric ratio, at the concentrations indicated by the solubility product, neglecting complicating factors such as the presence of other species which affect the solubility and phase chemistry. Deviations from stoichiometry reduce the volume fraction of precipitate available and excess of either solute will result in the formation of coarse particles. These particles may exert a limited boundary pinning effect but at a low efficiency in terms of the utilisation of the addition.

Figure 29 illustrates a further problem in the context of current low-activation compositions, namely that stoichiometric TaN formation

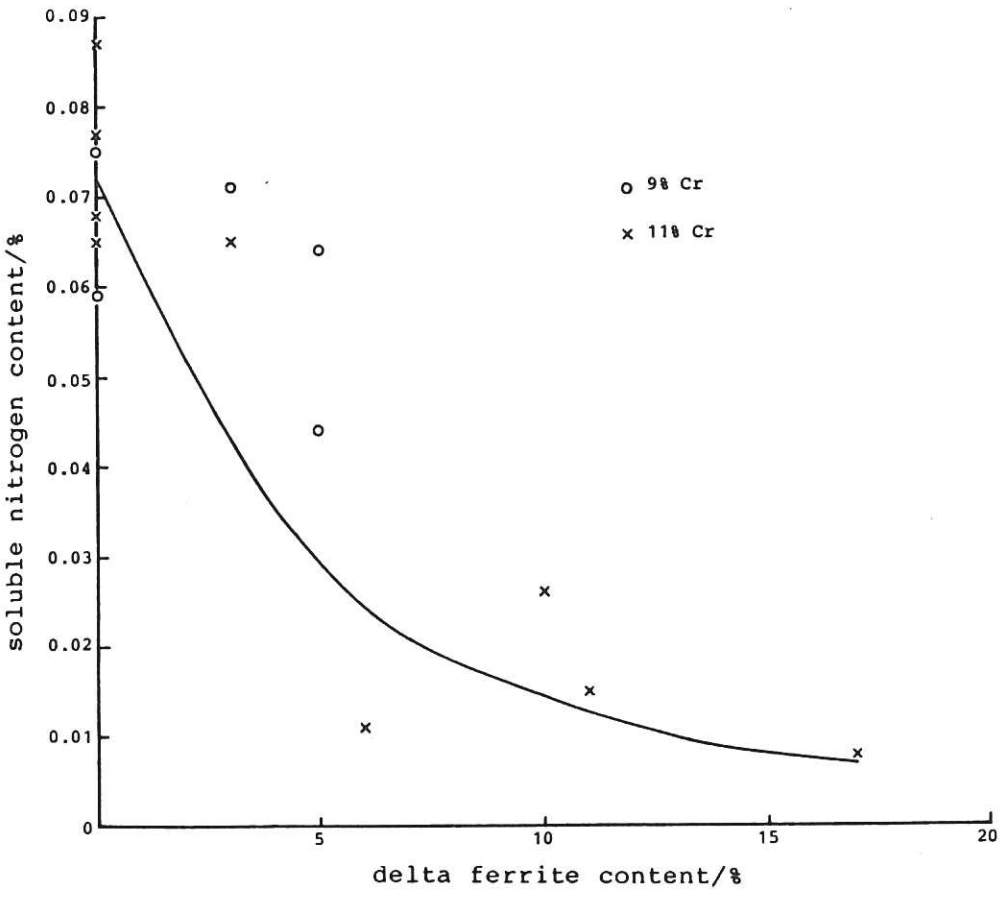

Fig.29 Graph showing the effect of soluble nitrogen content on the delta ferrite content

requires a relatively low nitrogen content, unless a comparatively coarse particle distribution can be tolerated. The nitrogen concentration of the current low-activation steels has been balanced against the need for austenite stability and for strength in the hardened and tempered condition. The phase stability may also be affected by the grain refining additions, since all of them are ferrite stabilisers.
The main objectives of the initial study of grain refinement were:

1. To determine the effectiveness of tantalum as a grain refiner under non-ideal conditions, where the additions were made to the current conpositions.

2. To examine the effect of the addition of tantalum on the austenite stability.

3. To examine the influence of tantalum additions in steels with reduced nitrogen content.

The LA7, LA13-type base compositions containing 0.25%V and 3.0%W were used to provide a constant reference matrix in the investigations.

5.1 Experimental methods

The investigation employed small experimental melts of 5kg mass, except for the casts designated 1107 and 1108, which had masses of 25kg. Problems of compositional control were encountered and some casts were used for the programme in the knowledge that the overall composition was not a good fit to the LA7-LA13 base, particularly in respect of the manganese and silicon contents.

To maintain a consistent identification system the LA7 and LA13 number has been retained for those casts corresponding to these compositions, with the addition of a suffix to denote varying levels of either or both tantalum or nitrogen. The compositions of the experimental casts are given in Table 11. All ingots were forged and hot rolled to 13 mm diameter bar, from which small lengths were cut for austenitising at temperatures between 1000° and 1200°C, before hardening to determine the prior austenite grain size and delta ferrite content within the martensitic structure.

5.2 Experimental findings

The measured grain sizes and delta ferrite contents of the grain-refined casts are shown in Table 11, together with the summary compositions. The steels are listed in approximately increasing order of tantalum and nitrogen contents. There was some variation in silicon and manganese contents and some variation in response to the austenitising treatments was noted. The difference in delta ferrite content between the LA7.1Ta steels may be attributed to their nitrogen contents. The LA7.1TaX and LA7.14TaX steels are so designated on account of their low silicon contents. It may be noted that they show a smaller degree of grain refinement and a slightly

Table 11

Composition, prior austenite grain size, hardness and delta ferrite content of tantalum-bearing experimental steels

cast no.	code	C	Si	Mn	Cr	V	W	N	Ta	austenitising temperature °C	ASTM grain size	hardness HV30	delta ferrite content
2224	LA7.1Ta (low N)	0.16	0.51	0.28	11.2	0.25	2.90	0.0087	0.10	1050	8½	440	19
										1100	8	432	17
2222	LA7.1Ta	0.16	0.47	0.25	11.3	0.22	2.91	0.093	0.07	1050	8½	527	0
										1100	8	529	0
2218	LA7.1Ta	0.17	0.08	0.28	11.1	0.21	2.93	0.07	0.092	1050	8½	480	5
										1100	7	477	3
2219	LA7.14Ta (low Si)	0.15	0.1	0.35	11.0	0.21	2.94	0.076	0.14	1050	6½	484	6
										1100	6	475	5
2223	LA7.2Ta	0.16	0.41	0.29	11.2	0.24	2.91	0.093	0.21	1050	8½	541	0
										1100	8½	539	0
1107	LA7.2Ta (int. N)	0.17	0.34	0.76	11.4	0.19	2.94	0.04	0.19	1000	10	488	11
										1050	9½	505	8
										1100	10	467	10
										1150	8 – 9½	468	12
										1200	8	465	13
1108	LA7.4Ta (int. N)	0.17	0.32	0.74	11.0	0.24	2.96	0.04	0.44	1100	9½ – 10	484	6
										1150	9	467	11
										1200	8	460	12
2216	LA13.1TaX	0.17	0.42	0.29	9.5	0.26	2.90	0.079	0.095	1050	8½	484	5
										1100	7	473	3
2220	LA13.1Ta	0.17	0.36	0.28	9.1	0.24	2.91	0.083	0.11	1050	7½	482	0
										1100	8	498	0
2221	LA13.2Ta	0.16	0.47	0.28	9.1	0.22	2.85	0.079	0.23	1050	8	480	0
										1100	8½	472	0
2217	LA13.2Ta (norm.Si)	0.17	0.27	0.40	9.1	0.23	2.93	0.058	0.19	1050	6½	490	6
										1100	6	481	5

CR 87.28/11

higher delta ferrite content at 1100°C than was observed with Steel LA7.1Ta.

The two LA7.2Ta steels again exhibited a significant degree of grain refinement in comparison with the LA7 base material, the steel with lower nitrogen content containing some delta ferrite. It may be noted that, at both tantalum concentrations, a slightly finer grain structure was found in the steels of higher delta ferrite contents. The LA7.4Ta material contained some delta ferrite with, again, effective grain refinement. The two LA13.1Ta steels were similar in composition and grain size, whereas the 9%Cr steels with 0.2% tantalum were less closely matched and showed a distinct difference in delta ferrite content.

The soluble tantalum and nitrogen concentrations were calculated for an 1100°C austenitising temperature and are correlated with the observed delta ferrite contents in Fig.29. Although there were some simultaneous variations in carbon, silicon and manganese contents the trend indicates a strong influence of the soluble nitrogen content on the incidence of delta ferrite. The effect of tantalum may be a contributing factor, as the steel with lowest soluble nitrogen content also had the highest calculated soluble tantalum content, at 0.08 mass percent. For most of the steels, however, the concentration lay below 0.01%.

The results indicate that tantalum additions confer a refinement of the prior austenite grain size for a range of tantalum and nitrogen contents. The formation of delta ferrite may be avoided, provided that the nitrogen content is kept up to at least 0.08%.

5.3 Discussion of grain size control

All the experimental tantalum-bearing steels had finer grain structures than the original LA7 and LA13 casts, though the degree of refinement varied. Figure 30 represents an attempt to systematise the observations and shows the change in prior austenite grain size for austenitising at 1100°C, as a function of the calculated insoluble tantalum content. The figures in brackets indicate the volume fraction of delta ferrite in the structures. No obvious relationship was found between the change in grain size and the soluble tantalum content.

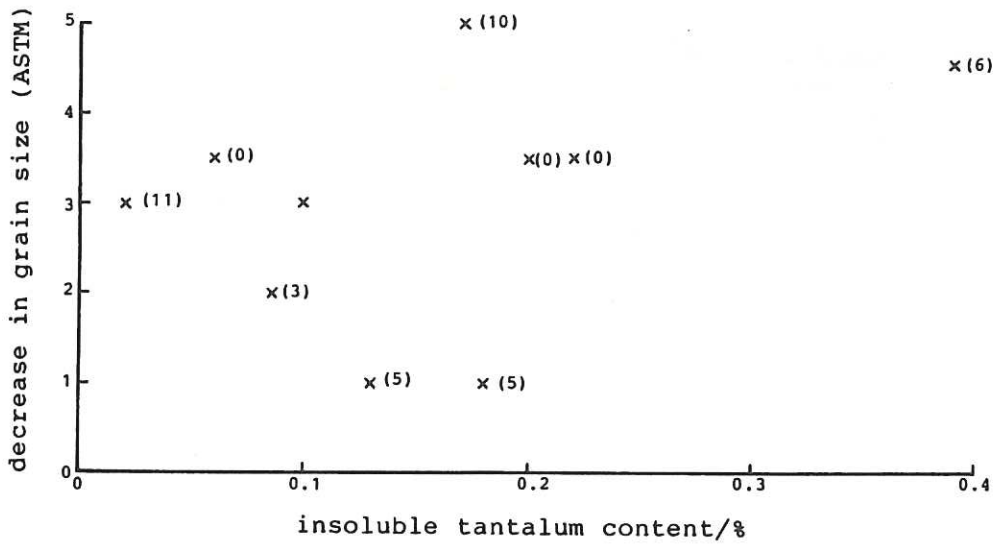

Fig.30 Graph showing the effect of insoluble tantalum and ferrite content on the decrease in grain size in comparison with alloys containing no tantalum. The values within parentheses indicate the percentage delta ferrite contents

The presence of delta ferrite in the steel with low nitrogen content may have confounded the effect of working with a near-stoichiometric ratio of Ta:N, at the solubility limit. The important finding, however, is that an adequate grain refining effect is obtainable from a tantalum addition at nitrogen contents sufficient to stabilise austenite in the LA7 composition.

The results suggest that an addition of at least 0.1% tantalum is required and that, unless there is a significant alteration in the composition, at least 0.08% nitrogen is required in both the 9%Cr and 11%Cr steels for austenite stability at 1100°C.

A decrease in the grain size with increasing insoluble tantalum content may be inferred if it is assumed that an increase in the delta ferrite content also has an associated grain refining effect. The results for the steels designated LA7.1TaX, LA7.14Ta and LA13.2TaX do not fit the overall pattern, however, so it is not possible to build a quantitative model to predict an optimum tantalum concentration from the present work. It is possible that the small change in grain size with tantalum additions in Steels LA7.1TaX and LA7.14Ta may be related to a change in the nature of the deoxidation product in the steel with the decrease in silicon content, such that their contribution to the grain refinement is weaker. This comment is, however, speculative. The main conclusion from the study is that a tantalum addition can yield a significant reduction in the prior austenite grain size, over a range of tantalum and nitrogen contents.

6. CONCLUSIONS AND SUGGESTIONS FOR FUTURE WORK

6.1 Welding response

The present investigations demonstrate that the basic LA7 steel can be welded using TIG methods and that it is necessary to control the formation of delta ferrite in the fusion zone.

It has been suggested [6] that a 9%Cr,Mo,Nb,V steel having elevated temperature properties slightly inferior to those of LA7 but comparable with those of 12%Cr,Mo,V steel can be welded into tube fabrications without a post-weld stress relief treatment. The present work indicates that this will not be possible with martensitic steels having the strength of LA7.

A more comprehensive examination of the welding response of the low-activation steels should be undertaken when the main line of their compositional development has been established.

6.2 Creep rupture properties

The observations on creep thus far indicate that both of the steels LA7 and LA13 will exhibit higher creep rates and, possibly, significantly lower rupture strengths than the FV448 reference steel. The results from the creep tests still in progress will show the degrees of creep strength and rupture ductility achievable in the high tungsten steels. Moreover, examination of the failed creep specimens should provide valuable information on the microstructures, since the exposure times when the creep tests are complete will be comparable with the anticipated service life.

6.3 Mechanical properties of selected low-activation steels

The current programme shows that 0.2% proof stresses in the region of 600 MPa at room temperature and 350MPa at 500°C are attainable with the vanadium-tungsten low-activation steels containing nominally 0.06% nitrogen. Data for selected alloys are summarised in Table 12.

Table 12

Summary of properties obtainable with low-activation V-W steels

Steel	temper	0.2% PS at 20°C	0.2% PS at 500°C	FATT °C
11Cr-0.25V-0.7W	2h at 750°C	565	340	+ 5
11Cr-0.25V-3.0W	2h at 750°C	620		+ 15
9Cr-0.25V-0.7W	2h at 750°C	535	350	+ 5

0055CR87.28/12

If it is assumed that a steel in the unirradiated condition would require an FATT close to or below room temperature, then the strengths of these candidate materials could be increased only if the toughness could be maintained at current levels since, as Table 12 shows, the FATT is already around room temperature. Some enhancement of the strength and toughness properties may be expected from the use of a grain refining addition and a beneficial effect on the FATT will result from a reduction of the phosphorus content from the current 0.010% maximum to about 0.005% maximum and of the sulphur content to 0.005% maximum.

The behaviour of LA8 steel, containing 0.46% vanadium, indicates that an increase in the vanadium content above the 0.25% level offers no advantage for strength at room or elevated temperatures after tempering at 750°C, though there is a slight benefit for the impact toughness.

Further work is needed to establish the optimum nitrogen concentration. For strength and control of the delta ferrite content it is desirable to maintain the current addition of about 0.05%. If this concentration needs to be reduced then some compensating addition of an austenite stabilising element would be required. The work so far suggests that the 'optimum' composition for further study and development would be based on the following constituents:

C	Si	S	P	Cr	V	Ta
0.16%	0.10%	0.005%(max)	0.005%(max)	9%	0.25%	0.12%

with the optimum concentrations of manganese, tungsten and nitrogen still to be established.

With the present nitrogen concentration, the basic properties and tempering response, in the temperature range 675°-750°C, could be determined for alloys with the tungsten content chosen in the range 0.7-3.0%, with

manganese at 0.8%, as employed in the earlier work. If it were considered preferable to work with a lower nitrogen content, of 0.005% for instance, then it would be necessary to select the tungsten and manganese concentrations to counter the effects of this reduction. It is tentatively suggested that with tungsten restricted to 1% or below, manganese contents up to 2% could be considered. The combined influence of the reduced nitrogen and tungsten contents would probably be a reduction in strength to below that of steel LA2.

6.4 Austenite grain size control

The observations show that grain refinement can be achieved through the addition of tantalum. The quantitative basis of the observations remains to be established and there appears to be a complicating factor in that the soluble nitrogen content of the present steels, possibly in interaction with the manganese component, has a strong influence on the incidence of delta ferrite formation. Nevertheless, it is evident that tantalum additions can bring about a worthwhile reduction in the prior austenite grain size, over a range of tantalum and nitrogen contents.

The possibility of utilising titanium as a grain refiner has not been explored in the present studies. Whilst there is no reason to believe that titanium will prove more effective than tantalum, the use of suitable additions could be investigated in future work, provided low nitrogen concentrations are selected. Because of the tendency to form an insoluble nitride, a titanium addition is unlikely to be effective if the nitrogen content is higher than about 0.01% and, for optimum grain refinement, nitrogen levels nearer to 0.005% would be preferred.

7. REFERENCES

1. K W Tupholme, D Dulieu and G J Butterworth, Investigations on low-activation 9 and 12%Cr,V,W steels for nuclear fusion reactor components, Culham Laboratory Report CLM-R271 (1986).

2. K Anderko, K David, W Ohly, M Schirra and C Wassilew, Optimisation work on niobium stabilised 12%CrMoVNb martensitic steels for breeder and fusion reactor applications, Conference on Ferritic Alloys for use in Nuclear Energy Technologies, Snowbird, Utah, June 1983.

3. T Gladman, On the theory of the effects of precipitate particles on grain growth in metals, Proc. Roy. Soc. 294A(1966)298.

4. C S Smith, Grains, phases and interfaces: An interpretation of microstructure, Trans. AIME 175(1948)15.

5. K Narita, Physical chemistry of the Groups 1Va (Ti,Zn), Va (V,Nb,Ta) and the rare earth elements in steel, Trans. ISIJ. 15(1975)145.

6. R Blount, Water Tube Boilermakers Association, private communication.

Available from
HER MAJESTY'S STATIONERY OFFICE
49 High Holborn, London, WC1V 6HB
(Personal callers only)
P.O. Box 276, London, SE1 9NH
(Trade orders by post)
13a Castle Street, Edinburgh, EH2 3AR
41 The Hayes, Cardiff, CF1 1JW
Princess Street, Manchester, M60 8AS
Southey House, Wine Street, Bristol, BS1 2BQ
258 Broad Street, Birmingham, B1 2HE
80 Chichester Street, Belfast, BT1 4JY

PRINTED IN ENGLAND